

---

Dissertations, Theses, and Masters Projects

Theses, Dissertations, & Master Projects

---

1975

## Composity particle reaction theory

John William Wilson

*College of William & Mary - Arts & Sciences*

Follow this and additional works at: <https://scholarworks.wm.edu/etd>

---

### Recommended Citation

Wilson, John William, "Composity particle reaction theory" (1975). *Dissertations, Theses, and Masters Projects*. Paper 1539623687.

<https://dx.doi.org/doi:10.21220/s2-3yfm-5p92>

This Dissertation is brought to you for free and open access by the Theses, Dissertations, & Master Projects at W&M ScholarWorks. It has been accepted for inclusion in Dissertations, Theses, and Masters Projects by an authorized administrator of W&M ScholarWorks. For more information, please contact [scholarworks@wm.edu](mailto:scholarworks@wm.edu).

## INFORMATION TO USERS

This material was produced from a microfilm copy of the original document. While the most advanced technological means to photograph and reproduce this document have been used, the quality is heavily dependent upon the quality of the original submitted.

The following explanation of techniques is provided to help you understand markings or patterns which may appear on this reproduction.

1. The sign or "target" for pages apparently lacking from the document photographed is "Missing Page(s)". If it was possible to obtain the missing page(s) or section, they are spliced into the film along with adjacent pages. This may have necessitated cutting thru an image and duplicating adjacent pages to insure you complete continuity.
2. When an image on the film is obliterated with a large round black mark, it is an indication that the photographer suspected that the copy may have moved during exposure and thus cause a blurred image. You will find a good image of the page in the adjacent frame.
3. When a map, drawing or chart, etc., was part of the material being photographed the photographer followed a definite method in "sectioning" the material. It is customary to begin photoing at the upper left hand corner of a large sheet and to continue photoing from left to right in equal sections with a small overlap. If necessary, sectioning is continued again - beginning below the first row and continuing on until complete.
4. The majority of users indicate that the textual content is of greatest value, however, a somewhat higher quality reproduction could be made from "photographs" if essential to the understanding of the dissertation. Silver prints of "photographs" may be ordered at additional charge by writing the Order Department, giving the catalog number, title, author and specific pages you wish reproduced.
5. PLEASE NOTE: Some pages may have indistinct print. Filmed as received.

**Xerox University Microfilms**

300 North Zeeb Road  
Ann Arbor, Michigan 48106

76-719

WILSON, John William, 1940-  
COMPOSITE PARTICLE REACTION THEORY.

The College of William and Mary in Virginia,  
Ph.D., 1975  
Physics, nuclear

**Xerox University Microfilms**, Ann Arbor, Michigan 48106

**COMPOSITE PARTICLE REACTION THEORY**

---

**A Dissertation**

**Presented to**

**The Faculty of the Department of Physics  
The College of William and Mary in Virginia**

**in Partial Fulfillment**

**Of the Requirements for the Degree of  
Doctor of Philosophy**

---

**by**

**John W. Wilson**

APPROVAL SHEET

This dissertation is submitted in partial fulfillment of  
the requirements for the degree of

Doctor of Philosophy

  
Author

Approved, June 1975

  
Carl E. Carlson

  
Franz L. Gross

  
William J. Kessler

  
Hans C. von Baeyer


  
Richard L. Kiefer  
Department of Chemistry

TABLE OF CONTENTS

	Page
ACKNOWLEDGMENTS. . . . .	iv
LIST OF FIGURES. . . . .	v
ABSTRACT . . . . .	vii
CHAPTER	
I. INTRODUCTION . . . . .	2
II. MULTIPLE SCATTERING THEORY. . . . .	15
III. THE OPTICAL MODEL. . . . .	22
IV. NUCLEAR SCATTERING. . . . .	33
1. GAUSSIAN MODEL CALCULATIONS . . . . .	34
2. SAXON-WOODS MODEL CALCULATIONS. . . . .	37
3. UNIFORM-DENSITY MODEL . . . . .	37
4. RESULTS . . . . .	39
V. CONCLUDING REMARKS . . . . .	45
APPENDIX . . . . .	48
BIBLIOGRAPHY . . . . .	60
VITA . . . . .	63

## ACKNOWLEDGMENTS

I thank Professor C. E. Carlson for his patience and encouragement during the course of this research and his very constructive criticism during manuscript preparation. The encouragement and understanding of my supervisors at Langley Research Center, especially Mr. George P. Wood and Dr. Frank Hohl, is gratefully acknowledged. I thank Professor G. S. Khandelwal and Dr. W. Meador for reviewing the manuscript during various stages of preparation. A special thanks to Dr. T. Foelsche who taught me of the problems associated with the radiation protection from heavy ions as encountered by high-altitude aircraft and spacecraft for which this work was initiated. A very special thank you to my wife without whose encouragement and understanding this thesis would have gone unfinished. Many thanks to Mrs. Dorothy Hicks for typing the manuscript. The research upon which this thesis is based was supported by the research programs of the National Aeronautics and Space Administration.

## LIST OF FIGURES

Figure	Page
1. Single scattering graph . . . . .	64
2. Rescattering graphs . . . . .	65
3. Nuclear root-mean-square radius as a function of mass number. Dashed curve is to guide the eye thru values used in calculations. Solid curve is used above $O^{16}$ . Dots are data tabulated by Hofstadter and Collard . . .	67
4. Nuclear half-density radius as a function of mass number. Solid curve is used above $He^4$ . Stars are values below $He^4$ obtained from assumed Gaussian density. Dots are data tabulated by Hofstadter and Collard. . . . .	68
5. Nuclear skin thickness as a function of mass number. Solid curve is used above $He^4$ . Dots are data tabulated by Hofstadter and Collard. . . . .	69
6. Total nucleon-nucleus cross section as a function of nuclear mass number for three model single-particle densities. Dots are data for neutron scattering at 1.064 GeV obtained by Schimmerling et al. . . . .	70
7. Nucleon-nucleus absorption cross section as a function of nuclear mass number for three model single-particle densities in comparison to experimental data at about 1 GeV. . . . .	71
8. Triton-nucleus absorption cross section as a function of target mass number for Saxon-Woods single-particle densities in comparison to measurements of Millburn et al. at 100 MeV/nucleon . . . . .	72
9. Oxygen-nucleus absorption cross sections as a function of target mass number for Saxon-Woods single-particle densities in comparison to measurements of Heckman et al. at 2.1 GeV/nucleon . . . . .	73
10. Total cross section as a function of projectile and target mass numbers for 1 GeV/nucleon using the Saxon-Woods single-particle densities . . . . .	74
11. Absorption cross section as a function of projectile and target mass numbers for 1 GeV/nucleon as calculated using Saxon-Woods single-particle densities . . . . .	75



Figure	Page
12. Average nuclear opacity as a function of projectile and target mass numbers for 1 GeV/nucleon as calculated using Saxon-Woods single-particle densities and equivalent uniform radii given by Hofstadter and Collard. . . . .	76
13. Absorption nuclear opacity as a function of projectile and target mass numbers for 1 GeV/nucleon as calculated using Saxon-Woods single-particle densities and equivalent uniform radii given by Hofstadter and Collard . . . .	77
14. Absorption to total cross section ratio as a function of projectile and target mass numbers for 1 GeV/nucleon . . . .	78
15. Factorizability as a function of projectile and target mass numbers for 1 GeV/nucleon . . . . .	79

## ABSTRACT

An effective potential operator is derived from the multiple-scattering series expansion of the exact transition amplitude for scattering two composite particles. This effective potential operator is used in a high-energy context to derive an approximate one-body Schroedinger equation by use of the closure approximation. The equivalent one-body equation is reduced to a set of coupled channel equations which relates the entrance channel to the final excited states of the projectile and target. A Schroedinger equation for the coherent elastic amplitude is extracted from the coupled equations. Total and absorption cross sections are derived on the basis of the eikonal approximation and the assumption that the coherent scattering dominates the elastic scattered amplitude. The equations are applied to the nuclear scattering problem and dependence of the total and the absorption cross sections on the model used for single particle densities is examined. The Saxon-Woods form factors show excellent agreement with neutron-nucleus cross sections. Absorption cross sections for heavy ion absorption on various target nuclei are calculated with some comparisons with the limited available experimental data. The use of geometric cross sections are found to be valid only when both target and projectile are heavier than argon at intermediate energies since nuclei show a rather high degree of transparency. Factorization of the total cross sections is found to be only in the limited geometric sense.

**COMPOSITE PARTICLE REACTION THEORY**

## I. INTRODUCTION

Most interactions to be observed in nature are among particles which are composed of some more fundamental constituents. This is obvious for atomic, molecular, and nuclear interactions in which constituents are sometimes ejected or transferred to change the basic makeup of the interacting particles. It is less obvious for the interaction of the so-called "elementary" particles of high-energy physics in particular, since the ejection of the more elementary stuff has either not been observed or not been properly recognized. Herein, we consider the interaction of composite particles in scattering states which are the states most accessible to experimental study. Our purpose will be to find relations between experimentally observable quantities for composite scattering in terms of physical quantities related to the internal constituents of which the composites are composed. In this paper, we will label as elementary those constituents of which a composite is composed and use the assumption that the number of elementary particles is conserved in the interaction. The composite particles are then bound collections of elementary particles. Although some of the bound states may be unstable, we will assume their lifetimes are long compared to the time in which the scattering systems interact.

Generally, the question of compositeness arises when a particle shows an internal structure so that its interaction appears not attributable to a potential emanating from a point. What appears instead are potentials emanating from the elemental constituents with the overall

interaction being composed of sums over potentials generated by individual constituents. The simplest form of such a potential is in electron scattering from nuclei in which the potential  $V(\vec{r})$  experienced by the electron is that generated by the charge distribution of protons  $\rho(\vec{r})$  in the nucleus as

$$V(\vec{r}) = \int \frac{\rho(\vec{x}) d^3x}{|\vec{r} - \vec{x}|}$$

The Fourier transform of  $\rho(\vec{x})$  is called the charge form factor. The phenomenology associated with electron scattering is to determine the charge distribution which most nearly represents the experimental electron cross sections.

An alternate but fully equivalent picture of the scattering of elementary projectiles with composite targets is to view the scattering in terms of the scattering of the projectile from individual constituents. Clearly, a principal contribution is made by the scattering of the projectile from a single constituent of the composite with such a contribution for each constituent. There are also terms contributed by scattering the projectile from two consecutive constituents with contribution from all possible constituent pairs. Similarly there are contributions from three, four, and more successive scatterings. Formalisms using this picture are called multiple-scattering theories.<sup>1-4</sup> It is clear from this description that the scattering from a composite target is determined from the relative positions of the constituents (i.e., the target wave function) and the amplitude for scattering the projectile from a single target constituent (i.e., a two-body scattering amplitude). The extension of multiple-scattering to treat composite projectiles

scattering from composite targets is reasonably straightforward and largely consists of finding the right bookkeeping formula to determine which constituent scattered from what constituent.<sup>5-9</sup>

An approximate multiple-scattering series can be derived on the basis of a small angle approximation.<sup>3</sup> The usual eikonal result<sup>10,11</sup> is a phase shift as a function of impact parameter given in terms of the interaction potential by

$$\chi(\vec{b}) = \frac{1}{\hbar v} \int_{-\infty}^{\infty} V(\vec{b} + \vec{z}) d\vec{z}$$

which is related to the scattering amplitude by

$$f(\vec{k}_f \cdot \vec{k}_i) = \frac{ik_i}{2\pi} \int e^{-i\vec{q} \cdot \vec{b}} d\vec{b}^2 \left\{ 1 - \exp[-i\chi(\vec{b})] \right\}$$

where  $\vec{k}_i$  and  $\vec{k}_f$  are the projectile initial and final momentum vectors,  $\vec{q}$  the momentum transfer, and  $v$  is the relative velocity. The usual Glauber<sup>3,4</sup> result for scattering an elementary projectile from a composite target is obtained by taking the interaction potential as

$$V(\vec{x}) = \sum_{\alpha} V_{\alpha}(\vec{x} - \vec{r}_{\alpha})$$

where  $\vec{x}$  is the position vector of the projectile relative to the target center of mass,  $\vec{r}_{\alpha}$  is the position vector of the  $\alpha$ -constituent of the target, and  $V_{\alpha}$  is the potential acting between the projectile and the  $\alpha$ -constituent.<sup>3,5,10</sup> The extension of Glauber theory for scattering two composite particles is accomplished by taking

$$V(\vec{x}) = \sum_{\alpha_j} V_{\alpha_j}(\vec{x} + \vec{r}_j - \vec{r}_{\alpha})$$

where  $\vec{r}_j$  is the location of the  $j$ -constituent of the projectile relative to the projectile center of mass.<sup>5-10</sup> The appropriate form for the scattering amplitude in Glauber theory is

$$f_{m\mu}(\vec{k}_f \cdot \vec{k}_i) = \frac{ik_i}{2\pi} \int d^3b e^{-i\vec{q} \cdot \vec{b}} \langle g_{T\mu}(\vec{\xi}_T) g_{Pm}(\vec{\xi}_P) | \Gamma(\vec{b}, \vec{\xi}_T, \vec{\xi}_P) | g_{T\alpha}(\vec{\xi}_T) g_{P\alpha}(\vec{\xi}_P) \rangle$$

where  $\vec{\xi}_P$  denotes the collection of projectile constituent relative coordinates  $\vec{r}_j$ ,  $\vec{\xi}_T$  denotes the collection of target constituent relative coordinates  $\vec{r}_\alpha$ , the  $g_{Pm}$  and  $g_{T\mu}$  are the internal wave functions of the projectile and target where  $m$  and  $\mu$  label the corresponding states, and the profile function is defined as

$$\Gamma(\vec{b}, \vec{\xi}_T, \vec{\xi}_P) = 1 - \exp[-i\chi(\vec{b}, \vec{\xi}_T, \vec{\xi}_P)]$$

Assuming the potentials  $V_{\alpha j}$  commute, the multiple-scattering form of the profile function is obtained as

$$\Gamma(\vec{b}, \vec{\xi}_T, \vec{\xi}_P) = 1 - \prod_{\alpha} \prod_j [1 - \gamma_{\alpha j}(\vec{b} + \vec{r}_j - \vec{r}_\alpha)]$$

where

$$\gamma_{\alpha j}(\vec{b} + \vec{r}_j - \vec{r}_\alpha) = 1 - \exp[-i\chi_{\alpha j}(\vec{b} + \vec{r}_j - \vec{r}_\alpha)]$$

and

$$\chi_{\alpha j}(\vec{x} + \vec{r}_j - \vec{r}_\alpha) = \frac{1}{kV} \int_{-\infty}^{\infty} V_{\alpha j}(\vec{b} + \vec{z} + \vec{r}_j - \vec{r}_\alpha) d\vec{z}$$

Note that  $\gamma_{\alpha j}$  is the profile function for scattering constituent  $\alpha$  with constituent  $j$  and could be obtained by laboratory measurement by using a beam of elementary type  $\alpha$  particles and a target of elementary type  $j$  particles (for example, a proton beam and hydrogen target to

obtain two-body data for nuclear scattering). The two-body scattering amplitude is given by

$$f_{\alpha_j}(\vec{q}) = \frac{ik_{\alpha_j}}{2\pi} \int e^{-i\vec{q}\cdot\vec{b}} d^2\vec{b} \gamma_{\alpha_j}(\vec{b})$$

which is related to the experimental cross sections by

$$\frac{d\sigma_{\alpha_j}}{d\Omega} = |f_{\alpha_j}(\vec{q})|^2$$

The profile function for composite scattering may now be written as a multiple-scattering series as (we now suppress the dependence on  $\vec{r}_j$  and  $\vec{r}_\alpha$  in the notation)

$$\Gamma(\vec{b}) = \sum_{\alpha_j} \gamma_{\alpha_j}(\vec{b}) - \sum_{\substack{\alpha_j \neq \beta_l \\ j \leq l}} \sum_{\beta_l} \gamma_{\alpha_j}(\vec{b}) \gamma_{\beta_l}(\vec{b}) + \dots$$

where the first term corresponds to the contributions in which only one constituent of the projectile scatters from only one constituent of the target (i.e., single scattering), the second term corresponds to events in which two successive scatterings between projectile and target constituents occur (i.e., double scattering) and the higher-order terms correspond to events in which three or more successive scatterings occur. The first two terms are graphically represented in figures 1 and 2. Two distinct graphs are required to represent the double-scattering term. Note also that the above Glauber form of the multiple-scattering series terminates after  $(A_p \cdot A_T)$  fold scattering terms where  $A_p$  is the number of projectile constituents and  $A_T$  is the number of target constituents. The Glauber theory accurately represents the composite scattering amplitude when the two-body scattering amplitudes are strongly peaked at small momentum transfer<sup>3,4,6</sup> although convergence of the Glauber



multiple-scattering series is slow when  $A_p$  and  $A_T$  are large.<sup>6,8,12</sup> As can be noted above, Glauber theory is straightforward although practical calculations are somewhat tedious when large numbers of constituents are involved.

Most calculations using Glauber theory have been for deuteron-deuteron scattering<sup>6,12-16</sup> and limited comparisons of the total cross section<sup>6</sup> and elastic differential cross section<sup>12</sup> with experiment are encouraging. Calculations of cross sections for various target and projectile nuclei have also been made<sup>7,8,12,16-19</sup> while comparison with experiments are lacking presumably due to the paucity of experimental data.

A useful phenomenological device for the analysis of composite particle scattering experiments is the optical model which is taken with a sufficient number of parameters so as to fit a large range of possible scattering data.<sup>20,21</sup> It is the complex valuedness of optical potentials which set them apart from a phenomenologically determined interaction potential. The name of this effective potential was chosen because of its analogy with the propagation of light through a semitransparent medium (i.e., complex index of refraction). The imaginary part of the optical potential corresponds to absorption of the incident beam by the medium (i.e., events in which the medium is changed or disturbed). By solving the optical model one obtains the elastic scattering amplitude from which the total cross section is calculated using the optical theorem and the absorption cross section is found by calculating the loss of elastically scattered particles. The spatial shape of the optical potential is usually assumed to represent the physical shape of

the target and projectile (i.e., related to the matter density) if the basic interaction of the elemental constituents is of short range.

A principal success of multiple-scattering theories is their ability to relate to the optical model.<sup>22,23</sup> This has allowed the optical potential for elementary projectile scattering from composite targets to be determined from the more fundamental quantities as the two-body scattering amplitude  $f(k, \vec{q})$  and the target single-particle density function given as

$$\rho(\vec{x}) = \frac{1}{A_T} \sum_{\alpha} \langle g_{T\alpha}(\vec{\xi}_T) | \delta(\vec{x} - \vec{r}_{\alpha}) | g_{T\alpha}(\vec{\xi}_T) \rangle$$

so that the optical potential is

$$V_{opt}(\vec{x}) \approx -\frac{2\pi}{\mu} f(k, \vec{0}) A_T \rho(\vec{x})$$

With this result, the optical model is removed from the sole position as a phenomenological tool to that of a first-principles theory for scattering an elementary projectile from a composite target. The advantage of the optical model is that the solution of an equivalent potential scattering problem is a less formidable task than computing each term of the multiple-scattering series when a large number of constituents are involved. An optical model for the scattering of a composite projectile from a composite target has been derived from Glauber's approximate form of multiple-scattering theory in the limit as either the target constituent number  $A_T$  or projectile constituent number  $A_p$  increase without bound provided  $A_T A_p \sigma = \text{constant}$  where  $\sigma$  is the total two-body cross section.<sup>8</sup> Although this restriction is not met in nature, this optical model has shown considerable success in analyzing elastic differential

cross-section data for alpha, carbon, and oxygen projectiles on the respective targets of iron, nickel, and carbon.<sup>24</sup> More recently, an extension of Watson's multiple-scattering series to the scattering of composite projectiles and targets indicates the optical model to be far more accurate than is found for the Glauber series.<sup>9</sup>

A principal aim in the study of composite scattering is in application to nuclear scattering. Motivated by the success of nuclear physics to explain many nuclear properties on the basis of nuclear models in which nuclei are to a good approximation bound collections of nucleons, we would expect the scattering states to be described within the same model, at least within appropriate limits. In that the physical domain probed by scattering experiments is generally different than those observed in nuclear experiments relating to deformations, low lying excited states, magnetic moment, etc., any systematic deviation from a composite scattering theory might be interpreted as inadequacy of the underlying nuclear model. All strongly interacting systems seem to be composite although the number of composite parts may not necessarily be fixed and a theory in which constituent number is emphasized may not be generally applicable.<sup>25</sup> However, if we consider the nearly 40 years of nuclear study, we are compelled to fix the constituent number in nuclear-scattering theory to be the baryon number of the systems as a first approximation.

Some ideas for the asymptotic behavior of composite nuclear scattering have been proposed by Chew on the basis of analytic S-matrix theory and assumed Regge behavior which states that at high energy and near

forward angles the scattering amplitude for two-body reactions has the form

$$F(s, t) \sim v_i(t) s^{\alpha_i(t)}$$

where  $s$  is the invariant mass squared,  $t$  is the square of the four momentum transfer, and  $\alpha_i(t)$  is the leading Regge trajectory (i.e., the Regge pole with largest real part of  $\alpha_i(t)$ ).<sup>25-27</sup> For elastic scattering, the leading trajectory is assumed to be the pomeron exchange pole for which  $\alpha_p(0) \approx 1$ . It has been shown that the asymptotic Regge term factorizes and the elastic amplitude for scattering A and B may be written as

$$F(s, t) \sim \gamma_{PA}(t) \gamma_{PB}(t) s^{\alpha_p(t)}$$

where  $\gamma_{PA}(t)$  and  $\gamma_{PB}(t)$  are the pomeron vertex functions.<sup>28,29</sup> As a consequence of this factorization and the optical theorem

$$\sigma_{AB} = -\frac{4\pi}{k} \text{Im}[F(s, 0)]$$

one has the result

$$\sigma_{AB}^2 = \sigma_{AA} \sigma_{BB}$$

Since scattering reactions for which all particles with baryon number less than 2 seem to exhibit Regge behavior, it is natural to expect this same asymptotic behavior in the nuclear case also<sup>25,26</sup> (i.e., involving a particle with baryon number of 2 or more). As noted above, a consequence of Regge behavior is the factorization of the asymptotic amplitude which leads to a simple experimental test. Chew further argues

that if the high energy limit is obtained relative to the level spacing of the composite structures then the asymptotic behavior may be obtained at present-day heavy ion accelerators.<sup>25</sup> Less optimistic are the results of Udgoankar and Gell-Mann who show on the basis of Glauber theory that the asymptotic region in the nuclear case lies above that obtained for particle physics.<sup>30</sup> The inherent simplicity of the factorization idea has brought renewed interest, (largely) in connection with the heavy ion experiments at the now defunct Princeton Particle Accelerator and the Bevalac. Several recent papers concerning factorization for nuclear cross sections have recently appeared.<sup>31-34</sup> Wang considers the factorization of heavy ion cross sections at energies of a few GeV/nucleon and found factorization not to apply.<sup>34</sup> Franco<sup>33</sup> did show that helium cross sections approach factorization for energies above about 50 GeV which generally agrees with the results of Udgoankar and Gell-Mann<sup>30</sup> and the results of Gribov.<sup>31</sup> Fishbane and Trefil<sup>32</sup> considered the optical model extension of Glauber theory proposed by Chou and Yang<sup>35</sup> within the context of gaussian matter density functions and observed a geometric form of factorization for composite projectiles and targets whenever the rms radii do not differ greatly. This geometric form of factorization is quite distinct from the original dynamical notion proposed by Gell-Mann,<sup>28</sup> Gribov and Pomeranchuk,<sup>29</sup> and Chew.<sup>25</sup>

It is the purpose of the present paper to examine a new multiple-scattering series for composite systems. We will concentrate on the exact scattering amplitude including all target recoil terms and not make forward scattering assumptions regarding the two-body scattering amplitudes as in the case of Glauber theory. The starting point is the N-body

time-dependent Schroedinger equation with two-body potentials and exact scattering amplitude. A multiple-scattering series is found for the exact amplitude.<sup>9</sup> This new series reduces to the usual Watson-multiple-scattering series when the projectile is elementary. The multiple-scattering series which converges to the exact amplitude is then compared to the Glauber series where the usual cancellation among principle value parts and higher-order terms is noted.<sup>9,10</sup> An effective potential relevant to the optical model is derived. Preliminary optical model considerations indicate that the coherent elastic scattering (scattering in which the projectile and target always remain in their ground state) should be well represented even when the constituent number is moderately small and the minimum model errors are obtained when the constituents are equally divided between the projectile and target indicating the optical model to be more accurate than heretofore expected. An approximate Lippmann-Schwinger equation (an integral form of the Schroedinger equation) in terms of the optical potential is derived and reduced to an equivalent Schroedinger equation for the scattering of a single particle in an energy-dependent local potential. Such a simplification is shown to result from a high-energy assumption and by application of the closure approximation to the accessible eigenstates of the target and the projectile. The elastic scattering potential is found to be the matrix element of the single-scattering operator taken between the ground states of the projectile and target. This result is obtained by projecting the coherent part of the scattered wave from the system's Lippmann-Schwinger equation. That the scattering should be dominated near the forward direction by the coherent amplitude follows since small momentum

transfer between constituents is not likely to excite the target or the projectile. This is surely not the case at large momentum transfer where incoherent scattering is expected to be an important if not the dominant contribution to the elastic channel. The sum effect of all incoherent (elastic and inelastic) processes is through the appearance of absorption in the forward scattered coherent amplitude and use of the optical theorem gives an estimate of the total cross section since coherent scattering dominates in the forward direction. Since incoherent processes are expected to be important only at large momentum transfer and since elastic scattering is very forward at high energy, we anticipate that the integrated coherent-elastic differential cross section (i.e., total coherent cross section) is a good estimate to the total elastic scattering cross section. We obtain good comparison with nuclear absorption experiments by using the difference between the total cross section and the total coherent cross section. The nuclear single particle densities are represented by three alternate models as a gaussian, Saxon-Woods function, and step function (uniform model). The Saxon-Woods density function is found to accurately represent the experimental scattering data.

The remainder of the paper is as follows: Chapter II contains a derivation of the multiple-scattering series, implications of the impulse approximation, relation to Glauber theory, and introduction of effective potential considerations. In Chapter III we derive an approximate Lippmann-Schwinger equation using the multiple-scattering formalism from which an equivalent one-body Schroedinger equation is found using a high-energy assumption and the closure approximation. A set of coupled

channel equations are then derived, from which the coherent elastic amplitude is extracted. The relation of the coherent elastic amplitude to the full coupled channel amplitude is discussed in an appendix. The optical potential for the coherent scattering is calculated and the total and absorption cross sections are found in terms of an eikonal approximation. In Chapter IV, the effects of models for the nuclear single-particle densities is examined for nucleon-nucleus scattering. The Saxon-Woods model is chosen for the calculation of cross sections as a function of projectile and target mass. Comparison of theoretical results using the Saxon-Woods model with heavy ion absorption experiments show good agreement. Results of the paper are discussed in Chapter V.



## II. MULTIPLE SCATTERING THEORY

We formulate a description of the experiment in which an energetic composite projectile of well defined momentum and mass number  $A_p$  strikes a composite target of mass number  $A_T$  and the scattered projectile is observed at some remote point from the target site. We assume the combined system of  $N$  constituents interacts through two-body potentials and the hamiltonian is given by

$$H = \sum_j T_j + \sum_{i < j} V_{ij} + \sum_\alpha T_\alpha + \sum_{\alpha < \beta} V_{\alpha\beta} + \sum_{\alpha j} V_{\alpha j} \quad (1)$$

where Roman subscripts pertain to the projectile and Greek subscripts refer to the target. The projectile hamiltonian can be reduced by extracting the center of mass motion as

$$H_p = \frac{1}{2mA_p} \vec{P}_p^2 + h_p \quad (2)$$

where the projectile momentum operator is

$$\vec{P}_p = \sum_j \vec{K}_j \quad (3)$$

and  $h_p$  depends on neither  $\vec{P}_p$  nor its canonically conjugate position variable. Similar results also obtain for the target

$$H_T = \frac{1}{2mA_T} \vec{P}_T^2 + h_T \quad (4)$$

with

$$\vec{P}_T = \sum_\alpha \vec{K}_\alpha \quad (5)$$

The full hamiltonian (1) can be written in the usual form showing explicitly the collective parts and interactions separately

$$H = \frac{1}{2mN} \vec{P}^2 + \frac{N}{2mA_p A_T} \vec{K}^2 + h_p + h_T + V \quad (6)$$

where the overall center of mass momentum operator is

$$\vec{P} = \vec{P}_p + \vec{P}_T \quad (7)$$

and the projectile momentum relative to the overall center of mass is

$$\vec{K} = \vec{P}_p - \frac{A_p}{N} \vec{P} = \frac{A_T}{N} \vec{P} - \vec{P}_T \quad (8)$$

and the interaction potential is

$$V = \sum_{\alpha_j} V_{\alpha_j} \quad (9)$$

The first term in Eq. (6), N-body center of mass motion energy, is completely decoupled from all of the remaining terms. The second term is the relative motion kinetic energy of the projectile and target. The projectile relative position variable appears only in the interaction term V. The projectile and target internal hamiltonians ( $h_p$  and  $h_T$ ) are coupled to the relative motion through the interaction V. As the projectile-target separation becomes large, the interaction term tends quickly to zero and we assume that well defined states of momentum are prepared in the entering state and are observed in the final state. These states are eigenstates of the free projectile-target hamiltonian

$$(H_p + H_T) \phi = E \phi \quad (10)$$

and can be decoupled into collective modes as can be seen from Eq. (6).

The full wave function satisfies the Schroedinger equation

$$H \Psi = E \Psi \quad (11)$$

and consist of a superposition of a free state plus a scattered state

$$\Psi = \phi + \Psi_{sc} \quad (12)$$

where

$$\Psi_{sc} = G \mathcal{T} \phi \quad (13)$$

with the Green's function given by

$$(E - H_p - H_r)^{-1} G = I \quad (14)$$

and transition operator

$$\mathcal{T} = V + V G \mathcal{T} \quad (15)$$

The usual wave operator which transforms free states to final scattered states is defined as

$$\Omega = \Omega \phi \quad (16)$$

and satisfies the Lippmann-Schwinger equation as

$$\Omega = I + G V \Omega \quad (17)$$

so that  $\mathcal{T}$  is formally given by

$$\mathcal{T} = V \Omega \quad (18)$$

It will be our purpose to find a series for  $\mathcal{T}$  that is in terms of simpler functions. The development follows closely the original work of Watson.<sup>1,2</sup>

To proceed with this program, we first define the transition operator for scattering the  $\alpha$ -constituent of the target with the  $j$ -constituent of the projectile which is a solution of a Lippmann-Schwinger type equation

$$t_{\alpha j} = V_{\alpha j} + V_{\alpha j} G t_{\alpha j} \quad (19)$$

and the wave operator which transforms the entering free state up to the collision of the  $\alpha$  and  $j$  constituents

$$\omega_{\alpha j} = 1 + \sum_{(pk) \neq (\alpha j)} G t_{pk} \omega_{pk} \quad (20)$$

Equation (20) is interpreted in the following way. The propagation to the time just before the  $\alpha$  and  $j$  constituents scatter is the sum of an operator which brings the initial free state plus the scattered part from the scattering of all other  $\beta$  and  $k$  constituents. We anticipate but must yet prove that the full wave operator consists of the wave operator which transforms the system to the  $\alpha$  and  $j$  collision, plus the additional contribution due to the scattering of the  $\alpha$  and  $j$  constituents; that is,

$$\Omega = \omega_{\alpha j} + G t_{\alpha j} \omega_{\alpha j} \quad (21)$$

which can be written in more symmetric fashion using Eq. (20) as

$$\Omega = 1 + \sum_{\alpha j} G t_{\alpha j} \omega_{\alpha j} \quad (22)$$

and we will now prove that the series given by equations (19) through (22) constitutes an exact representation of the scattering process defined by equations (1) through (18). Consider the product

$$\begin{aligned} V_{\alpha j} \Omega &= V_{\alpha j} \omega_{\alpha j} + V_{\alpha j} G t_{\alpha j} \omega_{\alpha j} \\ &= (V_{\alpha j} + V_{\alpha j} G t_{\alpha j}) \omega_{\alpha j} \\ &= t_{\alpha j} \omega_{\alpha j} \end{aligned} \quad (23)$$

Performing a summation on the  $\alpha$  and  $j$  constituents we obtain

$$\begin{aligned} \mathcal{J} &= \sum V_{\alpha j} \Omega \\ &= \sum t_{\alpha j} \omega_{\alpha j} \end{aligned} \quad (24)$$

which shows equations (19), (20), and (22) as a solution to (17).

The implied simplicity of the coupled equations (20) is somewhat misleading since the two-body scatterings represented by (19) are N-body operators. However, at sufficiently high energy, the effects of nuclear binding in Eq. (19) are negligible. The Green's function  $G$  may then be replaced by the free N-body Green's function  $G_0$  which satisfies

$$(E - \sum T_j - \sum T_\alpha) G_0 = I \quad (25)$$

The impulse approximation (Watson's form) consists of approximating Eq. (19) by

$$t_{\alpha j} = V_{\alpha j} + V_{\alpha j} G_0 t_{\alpha j} \quad (26)$$

so that the operator given by Eq. (26) acts as a true two-body transition amplitude.<sup>1,36</sup> The major advantage is that the amplitude (26) is closely related to the experimental nucleon-nucleon scattering amplitude which is reasonably well known and we will require no exact knowledge of the poorly understood two-body nuclear potential.

By iteration of equations (24) and (20) we obtain the multiple scattering series

$$\mathcal{J} = \sum_{\alpha_j} t_{\alpha_j} + \sum_{(\beta k) \neq (\alpha_j)} t_{\alpha_j} G t_{\beta k} + \dots \quad (27)$$

which constitutes a formal solution to the exact scattering problem.

If we now make the usual replacement<sup>1,36</sup> of

$$G \rightarrow G_0$$

where  $G_0$  is the free N-body Green's function, then the  $t_{\alpha_j}$  become essentially two-body operators and (27) becomes a series of sequential two-body operators. The graphical representations of the terms of the series (27) are shown in Figs. 1 and 2. The series (27) reduces to the usual Watson series when the projectile consists of a single particle.<sup>1,2</sup> When (27) is evaluated using the eikonal approximation,<sup>10</sup> the Glauber theory is obtained which implies cancellation of an infinity of terms of (27) in the eikonal context.<sup>9,37</sup>

The convergence of the multiple-scattering series (27) is not dependent on the strength of the two-body potentials which is its main advantage over the Born series. Unlike the generally singular two-body potentials, the two-body transition operators are finite everywhere so that the rates of convergence of the multiple-scattering series is fixed by the number of possible scattering combinations. For example, single scattering is composed of  $(A_T \cdot A_P)$  terms, double scattering has  $(A_T \cdot A_P)(A_T \cdot A_P - 1)$  terms, etc. Clearly, the convergence is slow when large numbers of nucleons are involved. Some of the practical aspects of convergence are discussed elsewhere within the context of the Glauber theory.<sup>8,12</sup> We will now use the multiple scattering series to derive an approximate scattering theory which shows promise in solving for the (approximate) scattering amplitude.

Before engaging in a full discussion of the optical model, we would first like to indicate how an effective potential description relates to the multiple-scattering series (27). To see this relation we seek a potential operator whose Born series is equivalent to the multiple-scattering expansion (27). Such an operator is closely related to the so-called optical potential<sup>20-23,38</sup> and we shall refer to it as  $V_{opt}$ . The transition operator

$$\mathcal{J}_{opt} = V_{opt} + V_{opt} G \mathcal{J}_{opt} \quad (28)$$

will be defined by

$$V_{opt} = \sum_{\alpha_j} t_{\alpha_j} \quad (29)$$

from which

$$\mathcal{J} = \mathcal{J}_{opt} - \sum_{\alpha_j} t_{\alpha_j} G t_{\alpha_j} - \dots \quad (30)$$

The optical model is obtained by retaining the first term in (30) and the order of approximation is

$$\mathcal{J}_{opt} - \mathcal{J} \approx V_{opt} G V_{opt} / (A_p A_T) \quad (31)$$

since  $t_{\alpha_j} \approx V_{opt} / (A_T A_p)$  where  $A_T$  and  $A_p$  are the mass numbers of the target and projectile, respectively. The amplitude (28) is a rather good approximation to the exact amplitude for light as well as heavy projectiles and targets. It is noted that for a fixed number of constituents that the minimum model error (31) occurs when constituents are equally divided among the projectile and target.

### III. THE OPTICAL MODEL

In the previous chapter, a multiple-scattering series was derived for the exact scattering amplitude. It is generally expected that the series will converge slowly so that direct summation of the series is not practical. It was noted that an effective potential could be found which accurately approximates the multiple scattering formalism and solution of the corresponding effective potential problem would, in effect, sum the multiple-scattering series to all orders. We will consider this possibility in more detail and show that the effective potential concept leads to an optical model of composite particle scattering.

Examination of the operators given by (20) and (22) shows that

$$\omega_{\beta k} = \Omega - G t_{\beta k} \omega_{\beta k} \quad (32)$$

with which Eq. (22) is rewritten as

$$\Omega = 1 + G \sum_{\alpha j} t_{\alpha j} \Omega - G \sum_{\alpha j} t_{\alpha j} G t_{\alpha j} \omega_{\alpha j} \quad (33)$$

We now consider the model in which we assume the wave operator to satisfy the approximate Lippmann-Schwinger equation

$$\Omega' = 1 + G V_{opt} \Omega' \quad (34)$$

where the effective potential is

$$V_{opt} = \sum_{\alpha j} t_{\alpha j} \quad (35)$$

and the lowest order correction to the model is



$$\Omega - \Omega' = O(1/A_p A_T) \quad (36)$$

as is evident from (33). To further simplify the Lippmann-Schwinger equation, we now examine the Green's function, G.

The Green's function with an outgoing spherical wave is

$$G = (E + i\eta - H_p - H_T)^{-1} \quad (37)$$

The eigenstates of the projectile hamiltonian of Eq. (2) are given by

$$H_p \phi_{m, \vec{k}}^P = (\epsilon_{\vec{k}}^P + \epsilon_m^P) \phi_{m, \vec{k}}^P \quad (38)$$

where  $\epsilon_m^P$  is the internal energy eigenvalue and the projectile kinetic energy is

$$\epsilon_{\vec{k}}^P = \frac{1}{2m A_p} \vec{k}^2 \quad (39)$$

with  $\vec{k}$  the eigenvalue of  $\vec{P}_p$  and similarly for the target hamiltonian of Eq. (4)

$$H_T \phi_{\mu, \vec{k}}^T = (\epsilon_{\vec{k}}^T + \epsilon_{\mu}^T) \phi_{\mu, \vec{k}}^T \quad (40)$$

with

$$\epsilon_{\vec{k}}^T = \frac{1}{2m A_T} \vec{k}^2 \quad (41)$$

and  $\vec{k}$  the eigenvalue of  $\vec{P}_T$ . The eigenstates of (38) and (40) are written as

$$\phi_{m, \vec{k}}^P = g_{P_m} \phi_{P_m \vec{k}} \quad (42)$$

and

$$\phi_{\mu, \vec{k}}^T = g_{T\mu} \phi_{T\vec{k}} \quad (43)$$

where the  $g$ 's denote the internal state and the  $\phi$ 's refer to one-body collective propagation and are of the form

$$\phi_{P\vec{k}} = \left(\frac{1}{2\pi}\right)^{\frac{3}{2}} \exp(i\vec{k} \cdot \vec{X}_P) \quad (44)$$

and similarly for the target. The product wave function is then

$$\begin{aligned} \phi_{m, \vec{k}}^P \phi_{\mu, \vec{k}}^T &= g_{Pm} g_{T\mu} \phi_{P\vec{k}} \phi_{T\vec{k}} \\ &= g_{Pm} g_{T\mu} \phi_{\vec{k}} \left(\frac{1}{2\pi}\right)^{\frac{3}{2}} \exp(i\vec{P} \cdot \vec{X}_{cm}) \end{aligned} \quad (45)$$

where

$$\phi_{\vec{k}} = \left(\frac{1}{2\pi}\right)^{\frac{3}{2}} \exp(i\vec{k} \cdot \vec{X}) \quad (46)$$

$\vec{X}_{cm}$  is the overall center of mass coordinate and  $\vec{X}$  is the relative coordinate between the projectile and target. In what follows, we will specialize to the overall center of mass frame in which

$$\vec{k} = -\vec{K} \quad (47)$$

and factor the center of mass motion from the state wave functions (45).

We then represent the Green's function as

$$G = \sum_{\vec{k}, m, \mu} \frac{|g_{Pm} g_{T\mu} \phi_{\vec{k}} \langle g_{Pm} g_{T\mu} \phi_{\vec{k}} |}{E + i\eta - \epsilon_m^P - \epsilon_\mu^T - \epsilon_{\vec{k}}^T} \quad (48)$$

where

$$\begin{aligned} \epsilon_{\vec{k}}^T &= \epsilon_{\vec{k}}^P + \epsilon_{\vec{k}}^T \\ &= \frac{N}{2mA_T A_P} \vec{k}^2 \end{aligned} \quad (49)$$

Rewriting the Lippmann-Schwinger equation (34) with use of (48) obtains

$$|\psi'\rangle = |g_p g_r \phi_k\rangle + \sum_{k_{m\mu}} |g_{p_m} g_{r_\mu} \phi_k\rangle [\epsilon_k + \epsilon_0 + \epsilon_0^T + i\eta - \epsilon_k^p - \epsilon_k^T - \epsilon_\mu^r]^{-1} \langle g_{p_m} g_{r_\mu} \phi_k | V_{opt} | \psi'\rangle \quad (50)$$

and in configuration space

$$\begin{aligned} \psi'(\vec{\xi}_p, \vec{\xi}_r, \vec{x}) &= g_p(\vec{\xi}_p) g_r(\vec{\xi}_r) \phi_k(\vec{x}) \\ &- \left( \frac{2m A_p A_r}{N} \right) \sum_{m\mu} \int d\vec{y} d^3\xi_p d^3\xi_r \frac{\exp[i k_{m\mu} |\vec{x} - \vec{y}|]}{4\pi |\vec{x} - \vec{y}|} \\ &\times g_{p_m}(\vec{\xi}_p) g_{r_\mu}(\vec{\xi}_r) g_{p_m}^+(\vec{\xi}_p') g_{r_\mu}^+(\vec{\xi}_r') V_{opt}(\vec{\xi}_p', \vec{\xi}_r', \vec{y}) \psi'(\vec{\xi}_p', \vec{\xi}_r', \vec{y}) \end{aligned} \quad (51)$$

where

$$\vec{\xi}_p = \{ \vec{r}_1, \vec{r}_2, \vec{r}_3, \dots, \vec{r}_{A_p} \} \quad (52)$$

$$\vec{\xi}_r = \{ \vec{r}_1, \vec{r}_2, \vec{r}_3, \dots, \vec{r}_{A_r} \} \quad (53)$$

and

$$\vec{k}_{m\mu}^2 = \vec{k}^2 + \left( \frac{2m A_p A_r}{N} \right) [(\epsilon_0^p - \epsilon_m^p) + (\epsilon_0^T - \epsilon_\mu^T)] \quad (54)$$

We now follow a development similar to that of Foldy and Walecka.<sup>38</sup>

If the energy transferred to the internal state of both the projectile and target are small compared to the incident energy, then

$$\vec{k}_{m\mu} \approx \vec{k}$$

We may now use the closure approximation to rewrite (51) as

$$\begin{aligned} \psi'(\vec{\xi}_p, \vec{\xi}_r, \vec{x}) &\approx g_p(\vec{\xi}_p) g_r(\vec{\xi}_r) \phi_k(\vec{x}) \\ &- \frac{1}{4\pi} \int d\vec{y} \frac{\exp(i k |\vec{x} - \vec{y}|)}{|\vec{x} - \vec{y}|} \left( \frac{2m A_p A_r}{N} \right) V_{opt}(\vec{\xi}_p, \vec{\xi}_r, \vec{y}) \psi'(\vec{\xi}_p, \vec{\xi}_r, \vec{y}) \end{aligned} \quad (55)$$

It follows that (55) satisfies an equivalent one-body Schroedinger

equation given by

$$(\nabla_{\vec{x}}^2 + \vec{k}^2) \psi'(\vec{\xi}_p, \vec{\xi}_T, \vec{x}) = \left( \frac{2m A_p A_T}{N} \right) V_{opt}(\vec{\xi}_p, \vec{\xi}_T, \vec{x}) \psi'(\vec{\xi}_p, \vec{\xi}_T, \vec{x}) \quad (56)$$

Note that the projectile and target constituent coordinates  $(\vec{\xi}_p, \vec{\xi}_T)$  appear as parameters in the equivalent one-body equations (55) and (56). The calculation of the asymptotic scattered wave is made as if the constituents are held fixed in their common center of mass frames.

The target and projectile internal wave functions are not eigenstates of the optical potential operator and the initial internal states are mixed into various modes of final excited internal states in the full scattered wave. This we express as

$$\psi'(\vec{\xi}_p, \vec{\xi}_T, \vec{x}) = \sum_{m, \mu} \psi_{m, \mu}(\vec{x}) g_{p_m}(\vec{\xi}_p) g_{T, \mu}(\vec{\xi}_T) \quad (57)$$

from which we write the coupled equations

$$(\nabla_{\vec{x}}^2 + \vec{k}^2) \psi_{m, \mu}(\vec{x}) = \left( \frac{2m A_p A_T}{N} \right) \sum_{m', \mu'} V_{m, \mu, m', \mu'}(\vec{x}) \psi_{m', \mu'}(\vec{x}) \quad (58)$$

where

$$V_{m, \mu, m', \mu'}(\vec{x}) = (g_{p_m} g_{T, \mu} | V_{opt}(\vec{\xi}_p, \vec{\xi}_T, \vec{x}) | g_{p_{m'}} g_{T, \mu'}) \quad (59)$$

The boundary condition for the elastic channel contribution is

$$\psi_{00}(\vec{x}) \sim \left( \frac{1}{2\pi} \right)^{\frac{3}{2}} \left[ \exp(i\vec{k} \cdot \vec{x}) + f_{00}(\hat{x}) \frac{\exp(ik|\vec{x}|)}{|\vec{x}|} \right] \quad (60)$$

and the inelastic channels satisfy

$$\psi_{m, \mu}(\vec{x}) \sim \left( \frac{1}{2\pi} \right)^{\frac{3}{2}} f_{m, \mu}(\hat{x}) \frac{\exp(ik|\vec{x}|)}{|\vec{x}|} \quad (61)$$

where  $m$  and  $\mu$  are not both zero. The optical model will be defined as the approximation of (58) for the elastic scattered part as

$$(\nabla_{\vec{x}}^2 + \vec{k}^2) \psi(\vec{x}) = \left( \frac{2m A_p A_T}{N} \right) W(\vec{x}) \psi(\vec{x}) \quad (62)$$

where

$$\psi(\vec{x}) \approx \psi_{00}(\vec{x}) \quad (63)$$

and

$$W(\vec{x}) = (g_p, g_{T_0} | V_{opt}(\vec{\xi}_p, \vec{\xi}_T, \vec{x}) | g_p, g_{T_0}) \quad (64)$$

with coupling to various excited internal states neglected. This is surely correct at small momentum transfer or near forward scattering. The corresponding approximate wave function is called the coherent scattered wave and it dominates the forward scattered component. We now evaluate the optical potential for use in the approximate Schroedinger equation (62). For simplicity, we first calculate the Fourier transform of a single term of (64) where the potential operator is given by (35)

$$(g_p, g_{T_0} | t_{\beta\ell}(k, \vec{q}) | g_p, g_{T_0}) = F_p(\vec{q}) F_T(\vec{q}) t_{\beta\ell}(k, \vec{q}) \quad (65)$$

where  $\vec{q}$  is the momentum transfer. Equation (65) is the well-known single-scattering term of the multiple-scattering series as expected. Note that  $t_{\beta\ell}$  is used to denote both the operator and its matrix elements and should cause no confusion. The form factors are the usual Fourier transforms of the single-particle density functions of the target and projectile. For the present, we treat the nucleon-nucleon interaction as being independent of constituent type (i.e., independent of  $\beta$  and  $\ell$ ). To account for constituent type dependence for nuclear scattering,  $t$  is understood to be the average amplitude

$$t = \frac{1}{A_p A_T} [N_p N_T t_{nn} + Z_p Z_T t_{pp} + (Z_p N_T + N_p Z_T) t_{np}] \quad (66)$$

where  $N_p$  and  $N_T$  are target and projectile neutron numbers and  $Z_p$  and  $Z_T$  are the corresponding proton numbers. Equation (66) reduces to the usual expression for an elementary projectile. The optical potential is found by taking the inverse Fourier transform of (65) and summing over constituents to obtain

$$W(\vec{x}) = A_p A_T \int d^3\vec{z} \rho_T(\vec{z}) \int d^3\vec{y} \rho_p(\vec{x} + \vec{z} + \vec{y}) \tilde{t}(k, \vec{y}) \quad (67)$$

where  $\rho_T$  and  $\rho_p$  are the target and projectile single-particle density functions and  $\tilde{t}(k, \vec{y})$  is the energy ( $k$ ) and space dependent two-body transition amplitude.

We use the usual parameterization of the two-body scattering amplitudes which satisfy unitarity, are customarily used to analyze experiments, and are consistent with Regge behavior as

$$f(e, \vec{q}) = \frac{\sqrt{me} \sigma(e)}{4\pi} [\alpha(e) + i] \exp[-\frac{1}{2} B(e) \vec{q}^2] \quad (68)$$

where  $e$  is the constituent energy in the two-body center of mass frame given in terms of relative velocity by

$$e = \frac{1}{2} \mu v^2 \quad (69)$$

where  $\mu = m/2$  is the two-body reduced mass and the relative velocity is

$$v = Nk / mA_p A_T \quad (70)$$

$\sigma(e)$  is the energy dependent total cross section,  $\alpha(e)$  is the energy

dependent ratio of real-to-imaginary part, and  $B(e)$  is an energy dependent parameter. The normalization of the transition amplitudes are such that

$$\tilde{t}(e, \vec{y}) = -\frac{1}{(2\pi)^3 \mu} \int \exp(i\vec{q} \cdot \vec{y}) f(e, \vec{q}) d^3\vec{q} \quad (71)$$

The space representation is given by

$$\tilde{t}(e, \vec{y}) = -\frac{\sqrt{me}}{m} \sigma(e) [\alpha(e) + i] [2\pi B(e)]^{-\frac{3}{2}} \exp[-\vec{y}^2/2B(e)] \quad (72)$$

for use in calculating the optical potential with Eq. (67). We note in passing that the two-body amplitude generally falls to zero in a short distance from its center at intermediate energies and the spatial variation of the single-particle density is slow in comparison and justifiably we can neglect the single-particle density variation over the two-body amplitude range as

$$W(\vec{x}) = A_p A_T \int d^3\vec{z} \rho_T(\vec{z}) \rho_p(\vec{x} + \vec{z}) \int d^3\vec{y} \tilde{t}(e, \vec{y}) + O[B(e)/(a_p^2 + a_T^2)] \quad (73)$$

where  $a_T$  ( $a_p$ ) is the target (projectile) rms radius. Considering for nuclear scattering that  $B(e)$  is on the order of  $0.3 \text{ fm}^2$  for energies from several hundred MeV to several GeV, the higher-order terms of (73) are small.

We must now solve the Schroedinger equation (62) for the optical potential given by (73), which we now write as

$$[\nabla_x^2 + k^2 - V(\vec{x})] \psi(\vec{x}) = 0 \quad (74)$$

where

$$V(\vec{x}) = \frac{2m A_p A_T}{N} W(\vec{x}) \quad (75)$$

We will require subsequently the maximum value of the potential which is

$$V(\vec{0}) \approx -\frac{2m}{r_0^3} \sqrt{\frac{E}{m}} \sigma(e) [\alpha(e) + i] \frac{A_p^2 A_T^2}{N(A_p^{3/2} + A_T^{3/2})^{3/2}} \quad (76)$$

where  $r_0 \approx 1.4$  fm.

We will solve Eq. (73) using the eikonal approximation which is valid for small angle scattering, provided that

$$|V(\vec{x})| \ll k^2 \quad (77a)$$

and

$$|\nabla_x V(\vec{x})| / |V(\vec{x})| \ll k \quad (78a)$$

Taking the total nucleon-nucleon cross section as 40 mb we find (77a) to be

$$k \gg 0.1 \text{ GeV}/c \quad (77b)$$

and (78a) is rewritten as

$$k \gg (a_p^2 + a_T^2)^{-1/2} \quad (78b)$$

and is easily met by (77b).

The fundamental quantity of the eikonal approximation is the phase function as function of impact parameter

$$\chi(\vec{b}) = -\frac{1}{2k} \int_{-\infty}^{\infty} V(\vec{b} + \vec{z}) d\vec{z} \quad (79)$$



In terms of the phase function we may calculate the scattering amplitude near forward angles by

$$f(\vec{k}_f \cdot \vec{k}) = -ik \int_0^{\infty} b db J_0(2kb \sin \frac{\theta}{2}) \{ \exp[i\chi(b)] - 1 \} \quad (80)$$

and from the optical theorem the total cross section

$$\begin{aligned} \sigma_T &= \frac{4\pi}{k} \text{Im}[f(\vec{k} \cdot \vec{k})] \\ &= 4\pi \int_0^{\infty} b db \left\{ 1 - \exp[-\chi_i(b)] \cos[\chi_r(b)] \right\} \end{aligned} \quad (81)$$

where  $\chi_r$  and  $\chi_i$  are the real and imaginary parts of the phase function (79). In that the number of angular momentum states which contribute to the elastic coherent cross section are large in accordance with inequality (78b), we may calculate the total coherent cross section from

$$\sigma_c = \int |f(\vec{k}_f \cdot \vec{k})|^2 d\Omega_f \quad (82)$$

which may be reduced to (c.f., ref. 11 on page 337)

$$\begin{aligned} \sigma_c &\approx 4\pi \int_0^{\infty} b db \left\{ 1 - \exp[-\chi_i(b)] \cos[\chi_r(b)] \right\} \\ &\quad - 2\pi \int_0^{\infty} b db \left\{ 1 - \exp[-2\chi_i(b)] \right\} \end{aligned} \quad (83)$$

by which we obtain the total incoherent cross section by

$$\begin{aligned} \sigma_{inc} &= \sigma_T - \sigma_c \\ &\approx 2\pi \int_0^{\infty} b db \left\{ 1 - \exp[-2\chi_i(b)] \right\} \end{aligned} \quad (84)$$

Since the coherent scattering dominates near forward angles where most of the elastic scattering occurs, we anticipate that the total coherent cross section would be a good approximation to the total (elastic) scattering cross section as

$$\sigma_s \approx \sigma_e \quad (85)$$

from which we find the total absorption cross section to be

$$\sigma_{abs} \approx \sigma_{inc} \quad (86)$$

The relation between the coherent, the elastic, the incoherent and the inelastic amplitudes are further discussed in appendix A. In discussing nuclear scattering in the next chapter, we will assume equations (83) to (86) are satisfied. We will justify this assumption by making a limited number of comparisons with laboratory experiments.

#### IV. NUCLEAR SCATTERING

It was shown in the previous chapter that the N-body scattering problem can be replaced by an optical model where the optical potential is related to the single-particle densities of the scattering composite systems and the two-body transition amplitudes. Particular advantage for this formalism lies in the fact that bound state wave functions required to calculate single-particle densities and the two-body scattering amplitudes required to compute the optical potential can be solved independently of the full N-body scattering process. Even more importantly, this same information required to determine the optical potential for heavy ion scattering is generally available from the totally independent set of experiments of electron scattering and nucleon-nucleon scattering. This last approach is quite attractive since aside from having a unifying effect on three otherwise loosely related disciplines, such a semi-empirical approach would provide a stringent consistency check on data obtained from three different unrelated experiments.

We derive in this chapter cross sections for nuclear scattering utilizing the data on nuclear radii compiled by Hofstadter et al. and two-body scattering found in nucleon-nucleon scattering experiments. Generally, among the best representations of nuclear single-particle densities is the Saxon-Woods function. However, the Saxon-Woods function is not amenable to analytic methods. For this reason we will consider two simpler functions for which the scattering cross sections can be reduced to a simple algebraic form. The three functions

considered for single-particle density models are (1) the gaussian function which shows a large degree of diffuseness with no well-defined nuclear surface, (2) the Saxon-Woods function with a nearly constant interior nuclear density with a reasonably defined but diffuse nuclear surface, and (3) the uniform density function with constant nuclear interior and a sharply-defined nuclear surface. We will evaluate the adequacy of these three models by comparing calculated results for the three models with measured total cross sections for neutron-nucleus scattering. Having examined the question of model dependence, we may then consider simultaneously to what extent does the coherent amplitude represent the elastic channel and how well does the eikonal approximation represent the elastic scattering amplitude. These questions will be examined by comparing optical model calculations with the eikonal approximation for absorption cross sections and comparing with nucleon-nucleus scattering experiments. Armed with the results of these comparisons, we then compare results for heavy ion absorption cross sections with the limited available experimental data. Cross sections for a selected set of possible projectiles are then presented for comparison with future experiments. We then make some observations about nuclear transparencies and a theoretical test of the factorization hypothesis proposed by Chew.

#### 1. Gaussian Model Calculations

We consider evaluation of the optical potential  $W(\vec{X})$  for the case when the two-body transition amplitude and the single-particle density functions are approximated by gaussian functions. The single-particle densities for a nucleus with  $A$  constituents we write as

$$\rho_A(\vec{r}) = \left(\frac{2}{3}\pi a_A^2\right)^{-\frac{3}{2}} \exp(-3\vec{r}^2/2a_A^2) \quad (87)$$

where  $a_A$  is the nuclear rms radius and the normalization is the usual

$$\int \rho_A(\vec{r}) d^3\vec{r} = 1 \quad (88)$$

The combined target-projectile overlap density is given by

$$\begin{aligned} \rho_N(\vec{r}) &= \int \rho_{A_T}(\vec{z}) \rho_{A_P}(\vec{r}+\vec{z}) d^3\vec{z} \\ &= \left(\frac{2}{3}\pi a_N^2\right)^{-\frac{3}{2}} \exp(-3\vec{r}^2/2a_N^2) \end{aligned} \quad (89)$$

where

$$a_N^2 = a_{A_P}^2 + a_{A_T}^2 \quad (90)$$

and  $a_A$  will be taken from the results compiled by Hofstadter.<sup>39</sup> We then find the optical potential to be

$$\begin{aligned} W(\vec{x}) &= -A_T A_P \sqrt{\frac{e}{m}} \sigma(e) [\alpha(e) + i] \left(\frac{2}{3}\pi a_V^2\right)^{-\frac{3}{2}} \exp(-3\vec{x}^2/2a_V^2) \\ &= -\frac{2\pi}{m} A_T A_P f(e, \vec{v}) \left(\frac{2}{3}\pi a_V^2\right)^{-\frac{3}{2}} \exp(-3\vec{x}^2/2a_V^2) \end{aligned} \quad (91)$$

where

$$a_V^2 = a_N^2 + 3B(e) \quad (92)$$

and  $\sigma(e)$  and  $\alpha(e)$  are given in equation (68). The Schroedinger equation (74) with the optical potential given by (75) will now be solved using the eikonal formalism.

First, we note the phase function can be written as

$$\chi(\vec{b}) = \chi_0 \exp(-3\vec{b}^2/2a_v^2) \quad (93)$$

where

$$\chi_0 = 3A_p A_T \sigma(e) [\alpha(e) + i] / 4\pi a_v^2 \quad (94)$$

The total cross section is found in terms of the phase function at zero impact parameter (94) as

$$\sigma_T = \frac{4}{3} \pi a_v^2 \operatorname{Re} [E_1(-i\chi_0) + \ln(-i\chi_0) + \gamma] \quad (95)$$

where  $\gamma$  is Euler's constant and  $E_1(z)$  is the exponential integral for complex argument. Similarly we find the incoherent cross section

$$\sigma_{inc} \approx \frac{2\pi}{3} a_v^2 [E_1(2\chi_{oi}) + \ln(2\chi_{oi}) + \gamma] \quad (96)$$

where

$$\chi_{oi} = d_m [\chi_0] \quad (97)$$

The rms radii for the electric charge distribution as taken from Hofstadter et al.<sup>39</sup> are given by

$$a_{\bar{K}} \left\{ \begin{array}{ll} 0.8 & A = 1 \\ 2.17 & = 2 \\ 1.78 & = 3 \\ 1.63 & = 4 \\ 2.4 & 6 \leq A \leq 14 \\ 0.82 A^{1/3} + 0.58 & A \geq 16 \end{array} \right\} \quad (\text{fm}) \quad (98)$$

and are shown in relation to the values obtained from electron scattering data in figure 3.

## 2. Saxon-Woods Model Calculations

The Saxon-Woods single-particle density is represented as

$$\rho(\vec{r}) = c / \{1 + \exp[(r - R)/c]\} \quad (99)$$

where the parameters  $R$  and  $c$  are given by

$$R = r_{0.5} \quad (100)$$

$$c = t/4.4 \quad (101)$$

and  $r_{0.5}$  is the radius at the half density and  $t$  is the skin thickness. Graphs of the half density radius and skin thickness are shown in figures 4 and 5 in comparison with the parameters as extracted from electron scattering data. For  $A$  less than 4 we use the gaussian densities of the previous section.<sup>39</sup>

The optical potential scattering for the Saxon-Woods form factors is not easily reducible to an analytic form and has been calculated here using numerical quadratures. A corresponding numerical evaluation of the phase function and forward scattered amplitude from which total cross sections and absorption cross sections are found has been made. The results will be discussed subsequently.

## 3. Uniform Density Model

We now derive expressions for the total and incoherent cross sections for scattering nucleons from a target nucleus with the single particle density approximated by a uniform distribution as given by

$$\rho(\vec{x}) = \rho_0 \theta(r_0 - |\vec{x}|) \quad (102)$$

where the equivalent uniform radius is

$$r_0 = 1.29 a_A \quad (103)$$

and

$$\rho_0 = 3/4\pi r_0^3 \quad (104)$$

where  $\theta(t)$  is the unit step function. The optical potential is

$$W(\vec{x}) = -A_T \sqrt{\frac{\epsilon}{m}} \sigma(e) [\alpha(e) + i] \rho_0 \theta(r_0 - |\vec{x}|) \quad (105)$$

with

$$V(\vec{x}) = \frac{-2m A_T^2}{1 + A_T} \sqrt{\frac{\epsilon}{m}} \sigma(e) [\alpha(e) + i] \theta(r_0 - |\vec{x}|) \quad (106)$$

The phase function is found to be

$$\chi(\vec{b}) = A_T \sigma(e) [\alpha(e) + i] \rho_0 \sqrt{r_0^2 - b^2} \quad (107)$$

from which we calculate the total cross section as

$$\begin{aligned} \sigma_T &= 4\pi \int_0^{r_0} b db [1 - \cos(\alpha a \sqrt{r_0^2 - b^2}) \exp(-a \sqrt{r_0^2 - b^2})] \\ &= 2\pi r_0^2 + \text{Re} \left\{ \frac{4\pi}{c^2} [(c r_0 + 1) \exp(-c r_0) - 1] \right\} \end{aligned} \quad (108)$$

where

$$a = A_T \rho_0 \sigma(e) \quad (109)$$

$$c = a + i a \alpha(e) \quad (110)$$

Similarly we find the incoherent cross section to be

$$\sigma_{inc} = \pi r_0^2 + \frac{\pi}{2a^2} [(2a r_0 + 1) \exp(-2a r_0) - 1] \quad (111)$$



We will not derive the general result for arbitrary target and projectile since it will not play a role in further development.

#### 4. Results

The total cross sections for nucleon-nucleus scattering using the gaussian, uniform, and Saxon-Woods single-particle densities with model parameters taken from the compilations of Hofstadter and Collard<sup>39</sup> are shown in Fig. 6 in comparison to the measurements of neutron-nucleus cross sections of Schimmerling et al. at 1.064 GeV.<sup>40,41</sup> The optical model shows remarkably good agreement with the experimental data when the Saxon-Woods model densities are chosen. The diffuseness of the gaussian density tends to overestimate the cross section while the sharp cutoff of the uniform model tends to underestimate the cross section. Even so, all three models give a reasonable representation of the data; the required radius to reproduce the data is slightly different for each model.

The absorption cross sections for nucleon-nucleus scattering as estimated by the total incoherent cross sections are shown in Fig. 7 as calculated for the three model densities. Also shown is the data from the experiments of Schimmerling et al.<sup>40,41</sup> at 1.064 GeV and of Igo et al.<sup>42,43</sup> at 1.0 GeV. Again, we see that all three models reasonably represent the data although there is a definite preference for the Saxon-Woods and gaussian results. Perhaps the most gratifying of these results is that the moderate sensitivity of the absorption cross section on variations in nuclear skin thickness as exhibited in the Saxon-Woods results appears to be displayed by the experimental data of Schimmerling et al. as well.

The Saxon-Woods functions appear most adequate to describe the nuclear single-particle densities, although the errors associated with gaussian and uniform models are usually less than 15 percent. The absorption cross sections for triton-nucleus scattering at 0.1 GeV/nucleon have been estimated by adjusting the two-body cross sections to 70 mb and using the gaussian density for the triton and Saxon-Woods for heavier nuclei. The results are shown in Fig. 8 in comparison with the data of Millburn et al.<sup>42,44</sup> Good agreement is displayed at lower target mass numbers with 30 percent errors for lead and uranium targets. The A dependence displayed by the experiments is nearly that of nucleon-nucleus cross sections. The theoretical A dependence of triton-nucleus scattering is markedly different than that obtained for nucleon-nucleus scattering.

Calculated oxygen-nucleus absorption cross sections at 2 GeV/nucleon are shown in Fig. 9 in comparison to the experiments of Heckman et al.<sup>45</sup> Excellent agreement is obtained for hydrogen and carbon targets. The results for sulfur differ by 17 percent while lead and copper are about 10 percent below the theoretical curve.

It is apparent from these limited comparisons that the simplified model derived in the previous chapter provides a reasonable representation of the experimental observations. Certainly in the case of nucleon-nucleus scattering the model is quite accurate. The triton-nucleus results are less convincing while the agreement with the more recent oxygen-nucleus data of Heckman et al. reassures us in the essential validity of the theory. In Figs. 10 and 11 we show calculations of

total and absorption cross sections for selected projectiles and energy of 1 GeV/nucleon. These results will hopefully be useful for comparison with future experiments.

An interesting quantity to be derived from the present calculations is the average nuclear opacity given by

$$O = \sigma_T / 2 \sigma_g \quad (112)$$

where the geometric cross section is given by

$$\sigma_g = \pi r_0^2 \quad (113)$$

and the equivalent uniform radius for the combined system in (113) is the sum of the equivalent uniform radii of the projectile and target. The opacity is shown in Fig. 12 for selected projectile masses as a function of target mass. The curves in the figure were hand drawn between the discrete target mass numbers. A rather surprising result is that all nuclei are more opaque to nucleons than to deuterons. This unusual transparency of the deuteron is due to the unusually low density of the deuteron; i.e., the deuteron consists of two nucleons spread over a region about the size of an oxygen nucleus. This yields an optical potential for deuteron-nucleus scattering which is rather shallow and spread over a large geometric region. As a consequence, only slight absorption of an incident deuteron beam occurs in the region of the potential. Elastic scattering which appears as diffraction to fill the hole formed in the incident beam by the optical potential requires the elastic cross section for deuterons to be small since the hole was left nearly filled by the shallow deuteron potential. This certainly confirms

our intuitive notion that the deuteron is easily destroyed in nuclear scattering since the deuteron is so weakly bound and can barely survive the shock. Had the optical potential been strongly absorbing (and hence deep) then we must conclude that diffraction effects are important and the elastic scattering cross section would be large, which disagrees with our notion that the deuteron breaks up easily in nuclear reaction. These ideas will be further discussed below.

We observe a general increase in opacity with increasing target mass as well as a small amplitude oscillation. The source of the oscillation can be seen in Figs. 3 to 5 as due to variations of diffuseness at the nuclear edge and the varying  $A$  dependence of the nuclear rms radius for light nuclei. The geometric limit for the cross sections are characterized by unit opacity, and is obtained only when both the projectile and target are relatively heavy. In most cases, the total cross section is less than twice the geometric cross section. However, the diffuse nuclear edge plays an ever-increasing important role for very heavy projectiles and targets. In no case is twice the geometric cross section exceeded by more than 10 percent. A related quantity is the absorption opacity defined as

$$O_{\text{abs}} = \sigma_{\text{abs}} / \sigma_g \quad (114)$$

The absorption opacity is shown in Fig. 13 for selected projectiles as a function of target mass number. The main features of the absorption opacity are its stronger dependence on variations in skin thickness and their larger values in comparison to average opacity.

The fact that nuclei are so transparent is in part the reason why absorption opacity is larger. Should nuclei appear as absorbing disk, then

$$\sigma_s \approx \sigma_{abs} \approx \sigma_e \quad (115)$$

in which case elastic scattering is purely diffractive. However, it is clear from our results that

$$\sigma_s < \sigma_{abs} \quad (116)$$

To further emphasize this point, we give the ratio  $\sigma_{abs}/\sigma_T$  in Fig. 14. It is clear that purely diffractive scattering is approached asymptotically for large target mass numbers but is not yet obtained for even uranium targets. It is seen from Fig. 14 that projectile-target interactions are quite inelastic except for heavy targets or projectiles.

We will now examine the proposal made by Chew that the scattering amplitude should factorize at energies which are large compared to the level spacing of internal excited states. Clearly, 1 GeV/nucleon fulfills this requirement for heavy ion scattering. We define the factorizability as the ratio

$$F_{PT} = \sigma_{PT}^2 / \sigma_{PP} \sigma_{TT} \quad (117)$$

where  $\sigma_{PT}$  is the total cross section for projectile denoted by P and target denoted by T. If Chew's proposal is correct then  $F_{PT}$  is independent of P and T and is equal to unity. We have calculated the factorizability for selected projectiles as a function of target mass number and the results are shown in Fig. 15. Clearly, factorization is obtained only in the region of the identity where the projectile and target are the same

$$F_{TT} = 1 \quad (118)$$

That is, factorization occurs only when the projectile and target have nearly the same number of constituents. This is clearly a geometrical form of factorization which occurs only when the projectile and target are of comparable size.<sup>32</sup> The dynamical factorization principle proposed by Chew is in disagreement with the present theory. We do expect factorization to be obtained at sufficiently high energy since nuclear matter is in that case unusually transparent and the Born approximation is expected to be accurate since shadow effects associated with multiple scattering are then small. The Born approximation is given by

$$f^B(q) = C A_P A_T F_P(q) F_T(q) t(k, q) \quad (119)$$

which is already in factorized form. Note, however, that this form of the factorization principle for heavy ion scattering requires much higher energies than that required to obtain factorization for nucleon-nucleon scattering.<sup>30, 31</sup>

## V. CONCLUDING REMARKS

A multiple-scattering series for heavy ion scattering has been derived which appears as a natural extension to the Watson formalism. The structure of this series indicates that it reduces to the Glauber result within the eikonal context. An effective potential operator was found which shows that an optical model for heavy ion scattering is a good approximation for even rather light nuclei. Using the multiple scattering formalism, an approximate Lippman-Schwinger equation was found for the effective potential. This Lippmann-Schwinger equation reduced to an approximate one-body Schroedinger equation for scattering in the effective potential when high-energy was assumed and the closure approximation was applied to the accessible eigenstates of the projectile and target. This equivalent one-body Schroedinger equation was shown to be equivalent to a set of coupled channel equations relating the entering state to all of the final channel states of this N-body system. The coherent elastic scattering was extracted by neglecting the coupling of the entering state to the various excited states of the target and projectile. The coherent scattering amplitude was solved using the eikonal approximation from which total cross sections are calculated. Model dependence for the nuclear form factors was examined by comparing with neutron-nucleus cross sections and the Saxon-Woods density function appears most appropriate. Further comparison of the incoherent cross sections for nucleon-nucleus scattering with experimental measurements of absorption cross sections shows remarkably good agreement, thus indi-

cating that most of the elastic scattering amplitude is well approximated by the eikonal solution of the coherent amplitude.

Calculations of nucleus-nucleus scattering were then made using the Saxon-Woods functions for scattering tritons and oxygen from various targets. Generally good agreement is obtained in comparison to absorption cross-section measurements. Additional calculations of scattering with selected projectiles were made for comparison with future experiments.

The theoretical results indicate that many target nuclei show an exceptional degree of transparency even for projectiles as heavy as oxygen with high opacity obtained mainly for both the projectile and target heavier than argon. Associated with this transparency is the tendency of these interactions to be inelastic. As the target and projectile mass increases the system appears more as an absorbing disk in which elastic scattering is purely diffractive. Although this limit can be approximated it is not yet obtained for uranium scattering from uranium.

Chew's suggestion that factorization may be obtained for nucleus-nucleus scattering at energies ( $\approx 1$  GeV) which are large compared to the nuclear level spacing is not supported by the present results. A geometric factorization principle similar to the results derived by Fishbane and Trefil is observed.

Although a reasonable step in developing theory for heavy ion reactions has been made, a considerable body of work remains and we will conclude this paper by noting some needed developments. The most conspicuous are the lack of symmetrization of the theory with respect



to identical particles and the neglect of spin effects. These effects may well be small at high enough energy. There is a need for inclusion of relativistic effects in the theory. There are further questions regarding the effects of incoherent processes especially for nonforward scattering. The main problem in treating the incoherent scattering is the typically large number of channels involved and will probably be handled ultimately using statistical models.

## APPENDIX

### COMPOSITE REACTION COUPLED CHANNEL AMPLITUDES

In this appendix, we will examine the solution of the coupled channel equations for composite particle scattering. Particular attention will be given to the relation between the coherent elastic scattered wave, the Born approximation, Chew's form of the impulse approximation, the distorted-wave Born approximation (DWBA), and various approximation procedures to the coupled equations. Finally, we will show how the coupled equations can be solved assuming small angle scattering and a simplified expression for the elastic and all of the inelastic scattering amplitudes will be derived. We will further discuss the usual use of the optical theorem to estimate total cross sections from the coherent elastic scattered wave and, in particular, shed some light on the reasons why this estimate of total cross section is so successful.

Coupled channel equations. The starting point for the present discussion is the coupled channel (Schroedinger) equation relating the entrance channel to all excited states of the target and projectile which was derived assuming high energy and closure for the accessible internal eigenstates of the target and projectile derived in Chapter III. These coupled equations are given

$$(\nabla_{\vec{x}}^2 + \vec{k}^2) \psi_{m\mu}(\vec{x}) = \left( \frac{2m A_p A_T}{N} \right) \sum_{m'\mu'} V_{m\mu, m'\mu'}(\vec{x}) \psi_{m'\mu'}(\vec{x}) \quad (1)$$

where subscripts  $m$  and  $\mu$  label the eigenstates of the projectile and target,  $A_p$  and  $A_T$  are projectile and target mass number,  $m$  is constituent mass,  $\vec{k}$  is projectile momentum relative to the center of mass,  $\vec{x}$  is the projectile position vector relative to the target, with

$$V_{m\mu, m'\mu'}(\vec{x}) = \langle g_{p_m}(\vec{\xi}_p) g_{T_\mu}(\vec{\xi}_T) | V_{opt}(\vec{\xi}_p, \vec{\xi}_T, \vec{x}) | g_{p_{m'}}(\vec{\xi}_p) g_{T_{\mu'}}(\vec{\xi}_T) \rangle \quad (2)$$

$g_{p_m}(\vec{\xi}_p)$  and  $g_{T_\mu}(\vec{\xi}_T)$  are the projectile and target internal wave functions,  $\vec{\xi}_p$  and  $\vec{\xi}_T$  are collections of internal coordinates of the projectile and target constituents,  $V_{opt}(\vec{\xi}_p, \vec{\xi}_T, \vec{x})$  is the effective potential operator derived in Chapter II and given by

$$V_{opt}(\vec{\xi}_p, \vec{\xi}_T, \vec{x}) = \sum_{\alpha_j} t_{\alpha_j}(\vec{x}_\alpha, \vec{x}_j) \quad (3)$$

where  $t_{\alpha_j}(\vec{x}_\alpha, \vec{x}_j)$  is the two-body transition operator for the  $j$ -constituent of the projectile at position  $\vec{x}_j$  and the  $\alpha$ -constituent of the target at  $\vec{x}_\alpha$  and  $N$  is the total constituent number

$$N = A_p + A_T \quad (4)$$

We simplify the notation by introducing the wave vector

$$\bar{\Psi}(\vec{x}) = \begin{bmatrix} \psi_{00}(\vec{x}) \\ \psi_{01}(\vec{x}) \\ \psi_{10}(\vec{x}) \\ \vdots \\ \vdots \end{bmatrix} \quad (5)$$

and the potential matrix

$$\bar{\mathcal{V}}(\vec{x}) = \left( \frac{2m A_p A_T}{N} \right) \begin{bmatrix} V_{00,00}(\vec{x}) & V_{00,01}(\vec{x}) & V_{00,10}(\vec{x}) & \cdot & \cdot & \cdot \\ V_{01,00}(\vec{x}) & V_{01,01}(\vec{x}) & V_{01,10}(\vec{x}) & \cdot & \cdot & \cdot \\ V_{10,00}(\vec{x}) & V_{10,01}(\vec{x}) & V_{10,10}(\vec{x}) & \cdot & \cdot & \cdot \\ V_{11,00}(\vec{x}) & V_{11,01}(\vec{x}) & V_{11,10}(\vec{x}) & \cdot & \cdot & \cdot \\ \vdots & \vdots & \vdots & \vdots & \vdots & \vdots \\ \vdots & \vdots & \vdots & \vdots & \vdots & \vdots \\ \vdots & \vdots & \vdots & \vdots & \vdots & \vdots \end{bmatrix} \quad (6)$$

The coupled equations are then written in matrix form as

$$(\nabla_x^2 + k^2) \bar{\Psi}(\vec{x}) = \bar{\mathcal{V}}(\vec{x}) \bar{\Psi}(\vec{x}) \quad (7)$$

for which we now seek approximations.

Born approximation. The Born approximation of the coupled equations is written as

$$f^{\theta}(\vec{q}) = -\frac{1}{4\pi} \int e^{i\vec{q}\cdot\vec{x}} \bar{\mathcal{V}}(\vec{x}) d^3x \quad (8)$$

which is a matrix of approximate scattering amplitudes relating all possible entrance channels to all possible final channel states. For example, diagonal elements relate to all possible elastic scatterings of the system where the elastic channel is defined by the entrance channel. Recalling the definition of the potential matrix in equation (2), we write

$$f_{m'\mu', m\mu}^{\theta}(\vec{q}) = -\frac{1}{4\pi} \left( \frac{2m A_p^2 A_T^2}{N} \right) F_{p m' m}(\vec{q}) F_{T \mu' \mu}(\vec{q}) t(k, \vec{q}) \quad (9)$$

where  $F_{P_{m'm}}(\vec{q})$  and  $F_{T_{\mu'\mu}}(\vec{q})$  are the projectile and target form factors. Equation (9) corresponds to a generalized version of Chew's impulse approximation<sup>46</sup> or single-scattering approximation.<sup>47</sup> This is consistent with the idea that solution of the optical model implicitly sums the multiple scattering corrections. As noted in Chapter II, the Born series is term-by-term equivalent to the multiple-scattering series.

It follows from the form of Eq. (9) that

$$f_{m'\mu',m\mu}^B(\vec{q}) \sim [\delta_{m'm} + a_{P_{l_p}} |\vec{q}|^{l_p}] [\delta_{\mu'\mu} + a_{T_{l_t}} |\vec{q}|^{l_t}] t(k, \vec{q}) \quad (10)$$

at small momentum transfer where

$$l_p = \text{Max} \{ |J_{m'} - J_m|, 1 \} \quad (11)$$

and

$$l_t = \text{Max} \{ |J_{\mu'} - J_{\mu}|, 1 \} \quad (12)$$

where  $J_{\mu'}, J_{\mu} (J_{m'}, J_m)$  are the internal angular momentum quantum numbers of the target (projectile) in the final and entering states, respectively. The  $a_{T_{l_t}}$  and  $a_{P_{l_p}}$  are the lowest order nonvanishing transition moments of the target and projectile, respectively. On the basis of the Born approximation, we see a very strong threshold effect on the various excitation processes which causes an ordering in the contribution of specific excitation channels in going from small to large momentum transfer. Clearly, at zero momentum transfer, only the elastic channel is open. As the momentum transfer increases, the single dipole transitions for either the target or projectile, but not both, are displayed first. Note that this severely restricts the accessible angular momentum states

in the excitation process. At slightly higher momentum transfer, coincident dipole transitions in projectile and target and single quadrupole transitions are in competition with and may eventually dominate the single dipole transitions at sufficiently high momentum transfer. Similarly at higher momentum transfer, transitions to higher angular momentum states are possible.

Perturbation expansion and DWBA. According to the above discussion, we see that over a restricted range of momentum transfer the off-diagonal elements of the "Born" matrix of scattering amplitudes are small compared to the elastic-scattering amplitudes for the various channels found along the diagonal. Noting that these amplitudes are proportional to the potential, we may consider the decomposition

$$\bar{v}(\vec{x}) = \bar{v}_d(\vec{x}) + \bar{v}_o(\vec{x}) \quad (13)$$

where  $\bar{v}_d(\vec{x})$  are the diagonal parts of  $\bar{v}(\vec{x})$  and  $\bar{v}_o(\vec{x})$  are the corresponding off-diagonal parts. Clearly, we may assume

$$\bar{v}_o(\vec{x}) \ll \bar{v}_d(\vec{x}) \quad (14)$$

in accordance with the above discussion. We will treat the off-diagonal contribution as a perturbation and consider the iterated solution.

We rewrite Eq. (7) as

$$[\nabla_x^2 + k^2 - \bar{v}_d(\vec{x})] \bar{\psi}(\vec{x}) = \bar{v}_o(\vec{x}) \bar{\psi}(\vec{x}) \quad (15)$$

and take as a first approximation

$$[\nabla_x^2 + k^2 - \bar{v}_d(\vec{x})] \bar{\psi}_0(\vec{x}) = 0 \quad (16)$$

The only nonzero component of  $\bar{\psi}_0(\vec{x})$  is the elastic coherent scattered wave. If the initial prepared states are in their ground states, then we solve for the coherent elastic wave from

$$(\nabla_x^2 + \vec{k}^2) \psi_c(\vec{x}) = \mathcal{V}_{o,o,o}(\vec{x}) \psi_c(\vec{x}) \quad (17)$$

and the first approximation is

$$\bar{\psi}_0(\vec{x}) = \begin{bmatrix} \psi_c(\vec{x}) \\ 0 \\ 0 \\ \vdots \end{bmatrix} \quad (18)$$

Estimating the perturbation via use of Eq. (18) we now correct the result as

$$[\nabla_x^2 + \vec{k}^2 - \bar{\mathcal{V}}_d(\vec{x})] \bar{\psi}^{(1)}(\vec{x}) = \bar{\mathcal{V}}_o(\vec{x}) \bar{\psi}_0(\vec{x}) \quad (19)$$

The right-hand side is a term describing the source of excitation caused by the interaction of the coherent amplitude and is of the form

$$\bar{\mathcal{V}}_o(\vec{x}) \bar{\psi}_0(\vec{x}) = \begin{bmatrix} 0 \\ \mathcal{V}_{o1,o,o} \\ \mathcal{V}_{o2,o,o} \\ \vdots \end{bmatrix} \psi_c(\vec{x}) \quad (20)$$

Noting that the first component of the source of excitation is zero, we see that the equation for the first component of Eq. (19) is

$$[\nabla_x^2 + \vec{k}^2 - \mathcal{V}_{o,o,o}(\vec{x})] \psi_{o,o}^{(1)}(\vec{x}) = 0 \quad (21)$$

from which we see that the iteration of the elastic channel obtains again the coherent elastic amplitude

$$\psi_{o,o}^{(1)}(\vec{x}) = \psi_c(\vec{x}) \quad (22)$$

The remaining components of (19) are

$$[\nabla_x^2 + \vec{k}^2 - \mathcal{V}_{m\mu, m\mu}(\vec{x})] \psi_{m\mu}^{(i)}(\vec{x}) = \mathcal{V}_{m\mu, 00}(\vec{x}) \psi_c(\vec{x}) \quad (23)$$

This process of successive iteration is equivalent to the series approximation

$$\bar{\psi}(\vec{x}) = \bar{\psi}_0(\vec{x}) + \bar{\psi}_1(\vec{x}) + \bar{\psi}_2(\vec{x}) + \dots \quad (24)$$

where

$$[\nabla_x^2 + \vec{k}^2 - \bar{\mathcal{V}}_d(\vec{x})] \bar{\psi}_0(\vec{x}) = 0 \quad (25)$$

and

$$[\nabla_x^2 + \vec{k}^2 - \bar{\mathcal{V}}_d(\vec{x})] \bar{\psi}_i(\vec{x}) = \bar{\mathcal{V}}_0(\vec{x}) \bar{\psi}_{i-1}(\vec{x}) \quad (26)$$

The iterated solution and series solution are related as

$$\bar{\psi}_i(\vec{x}) = \bar{\psi}^{(i)}(\vec{x}) - \bar{\psi}^{(i-1)}(\vec{x}) \quad (27)$$

and the  $i^{\text{th}}$  iterate is the  $i^{\text{th}}$  partial sum of the series.

Further insight can be gained by considering the formal solution to the coupled equations (25) and (26). We introduce the diagonal coherent propagator

$$G_c = [\nabla_x^2 + \vec{k}^2 - \bar{\mathcal{V}}_d(\vec{x})]^{-1} \quad (28)$$

and the coherent wave operator

$$\Omega_c = 1 + (\nabla_x^2 + \vec{k}^2)^{-1} \bar{\mathcal{V}}_d(\vec{x}) \quad (29)$$

with which the solution to Eq. (26) is written as



$$\bar{\psi}_i(\vec{x}) = G_c \bar{v}_0(\vec{x}) \bar{\psi}_{i-1}(\vec{x}) \quad (30)$$

and note that

$$\bar{\psi}_0(\vec{x}) = \Omega_c \bar{\psi}_p(\vec{x}) \quad (31)$$

where  $\bar{\psi}_p$  is the entering plane-wave state. The series (24) may now be written as

$$\begin{aligned} \bar{\psi} &= \Omega_c \bar{\psi}_p + G_c \bar{v}_0 \Omega_c \bar{\psi}_p + G_c \bar{v}_0 G_c \bar{v}_0 \Omega_c \bar{\psi}_p + \dots \\ &= \Omega \bar{\psi}_p \end{aligned} \quad (32)$$

The first term is the coherent elastic scattered wave as noted above and represents attenuation and propagation of the incident plane wave in matter. Since  $\Omega_c$  is diagonal, this propagation is in undisturbed matter. The second term relates to the excitation caused by the presence of the coherent elastic wave followed by coherent propagation in disturbed matter. Note that the second term has no contribution in the elastic channel. The third term relates to further excitation caused by the presence of the scattered waves formed exclusively by coherent excitation and the first correction to the elastic channel due to incoherent processes. Hence, the coherent elastic wave is correct up to third-order terms in off-diagonal elements of the potential matrix which shows considerable damping or suppression at small momentum transfer as shown in connection with Eq. (10). This may well be the reason why the coherent elastic amplitude has been so successful in nuclear applications<sup>48</sup> as shown in Chapter IV.

It is obvious from the structure of the second term in the series (32), that it is the usual distorted-wave Born approximation<sup>49</sup> or single inelastic scattering approximation<sup>50</sup> and the entire series could be

aply referred to as the distorted-wave Born series. However, recalling that the terms of the series correspond to a successively larger number of changes in states of excitation (i.e., the first term contains no excitation, the second term transforms the coherent elastic wave to the excited states, the third term transforms the excited states of the second term to new excitation levels and so on); a more appropriate name for the series would be the "multiple excitation series."

Full coupled channel amplitudes. We consider now the solution to the coupled equations (7) within a small-angle approximation. We will in effect sum the multiple excitation series to all orders and as a final result give expressions for the scattering amplitudes connecting all possible entrance channels to all possible final channels. Making now the forward scattering assumption, we take the boundary condition as

$$\lim_{z \rightarrow -\infty} \bar{\psi}(\vec{x}) = \left(\frac{1}{2\pi}\right)^{\frac{1}{2}} \exp(i\vec{k}\cdot\vec{x}) \bar{\delta} \quad (33)$$

where  $-\hat{z}$  is the direction to the beam source and  $\bar{\delta}$  is a constant vector with a unit entry at the entrance channel element and zero elsewhere. Equation (33) simply states that no particles are scattered backwards. Physically, this assumption is justified since the backward scattered component for most high-energy scattering is many orders of magnitude less than the forward scattered component. We will seek a solution to Eq. (7) of the form

$$\bar{\psi}(\vec{x}) = \left(\frac{1}{2\pi}\right)^{\frac{1}{2}} \exp[i\bar{\phi}(\vec{x})] \exp(i\vec{k}\cdot\vec{x}) \bar{\delta} \quad (34)$$

where  $\bar{\phi}(\vec{x})$  is a matrix with elements connecting all possible entrance

channels to all possible final channels. The boundary condition (33) implies

$$\lim_{z \rightarrow -\infty} \bar{\phi}(\vec{x}) = 0 \quad (35)$$

as a boundary condition on  $\bar{\phi}(\vec{x})$ . Using Eq. (34) we may write an equation for  $\bar{\phi}(\vec{x})$  as

$$i \nabla_x \bar{\phi}(\vec{x}) - [\nabla_x \bar{\phi}(\vec{x})]^2 - 2 \vec{k} \cdot \nabla_x \bar{\phi}(\vec{x}) - \bar{V}(\vec{x}) = 0 \quad (36)$$

If  $\bar{V}(\vec{x})$  is small compared to the kinetic energy

$$\bar{V}(\vec{x}) \ll k^2 \quad (37)$$

and if the change in  $\bar{V}(\vec{x})$  is small over one oscillation of the incident wave as

$$\nabla_x \bar{V}(\vec{x}) \ll k \bar{V}(\vec{x}) \quad (38)$$

where inequalities refer to magnitudes of elements on each side of (37) and (38); then we may approximate (36) by

$$2k \frac{\partial}{\partial z} \bar{\phi}(\vec{x}) = -\bar{V}(\vec{x}) \quad (39)$$

which has a solution as

$$\bar{\phi}(\vec{x}) = -\frac{1}{2k} \int_a^z \bar{V}(\vec{x}') d\vec{x}' \quad (40)$$

where the value  $a$  is fixed by the boundary condition (35) to be  $-\infty$ .

We may now write the scattered wave (34) as

$$\bar{\psi}(\vec{x}) = \left(\frac{1}{2\pi}\right)^{\frac{1}{2}} \exp\left[-\frac{i}{2k} \int_{-\infty}^z \bar{V}(\vec{x}') d\vec{x}'\right] \exp(i\vec{k} \cdot \vec{x}) \delta \quad (41)$$

We note that the wave operator is approximated by

$$\Omega \approx \exp\left[-\frac{i}{2k} \int_{-\infty}^{\infty} \bar{V}(\vec{x}') d\vec{x}'\right] \quad (42)$$

The scattering amplitudes are given by

$$\begin{aligned} \bar{f}(\vec{q}) \bar{\delta} &= -\sqrt{\frac{\mu}{2}} \int \exp(-i\vec{k}_f \cdot \vec{x}) \bar{V}(\vec{x}) \bar{\psi}(\vec{x}) d^3\vec{x} \\ &= -\frac{1}{4\pi} \int \exp(-i\vec{q} \cdot \vec{x}) \bar{V}(\vec{x}) \exp\left[\frac{i}{2k} \int_{-\infty}^{\infty} \bar{V}(\vec{x}') d\vec{x}'\right] \bar{\delta} d^3\vec{x} \end{aligned} \quad (43)$$

where  $\vec{k}_f$  is the final projectile momentum and  $\vec{q}$  the momentum transfer is given by

$$\vec{q} = \vec{k}_f - \vec{k} \quad (44)$$

We define a cylindrical coordinate system with cylinder axis along the beam direction and write

$$\vec{x} = \vec{b} + \vec{z} \quad (45)$$

where  $\vec{b}$  is the impact parameter vector and note that

$$\vec{q} \cdot \vec{x} = \vec{q} \cdot \vec{b} + O(\theta^2) \quad (46)$$

where  $\theta$  is the scattering angle which we assume small. Using then the small angle approximation we obtain

$$\bar{f}(\vec{q}) = -\frac{1}{4\pi} \int \exp(-i\vec{q} \cdot \vec{b}) \bar{V}(\vec{b} + \vec{z}) \exp\left[-\frac{i}{2k} \int_{-\infty}^{\infty} \bar{V}(\vec{b} + \vec{z}') d\vec{z}'\right] d^2\vec{b} dz \quad (47)$$

which we rewrite as

$$\bar{f}(\vec{q}) = -\frac{ik}{2\pi} \int \exp(-i\vec{q} \cdot \vec{b}) \left\{ \exp[i\bar{\chi}(\vec{b})] - 1 \right\} d^2\vec{b} \quad (48)$$

where

$$\bar{\chi}(\vec{b}) = -\frac{1}{2k} \int_{-\infty}^{\infty} \bar{V}(\vec{b} + \vec{z}) d\vec{z} \quad (49)$$

Equation (48) gives the matrix of scattering amplitudes of all possible entrance channels to all possible final channels of the system.

We may inquire as to the relation between the eikonal result for the full scattering amplitude (48) and the various approximate results discussed earlier in this appendix. First, we consider the expansion in powers of  $\bar{\chi}$  of the integrand of equation (48)

$$\bar{f}(\vec{q}) = -\frac{ik}{2\pi} \int e^{i\vec{q}\cdot\vec{b}} \left[ i\bar{\chi} - \frac{1}{2}\bar{\chi}^2 - \frac{1}{3!}i\bar{\chi}^3 + \dots \right] d^2\vec{b} \quad (50)$$

The first term is the Born approximation at small angles. Higher-order terms are multiple-scattering corrections to the Born result. Recall that the Born approximation for the optical potential is equivalent to Chew's impulse approximation. A more interesting result is obtained by separating the  $\bar{\chi}$  matrix into its diagonal and off-diagonal parts as

$$\bar{\chi}(\vec{b}) = \bar{\chi}_d(\vec{b}) + \bar{\chi}_o(\vec{b}) \quad (51)$$

which corresponds to the diagonal and off-diagonal parts of the matrix potential  $\bar{V}(\vec{x})$ . If we now make an expansion in powers of the off-diagonal part of  $\bar{\chi}$  in equation (48) we obtain

$$\begin{aligned} \bar{f}(\vec{q}) = & -\frac{ik}{2\pi} \int e^{i\vec{q}\cdot\vec{b}} \left[ \exp(i\bar{\chi}_d(\vec{b})) - 1 \right] d^2\vec{b} \\ & - \frac{ik}{2\pi} \int e^{-i\vec{q}\cdot\vec{b}} e^{i\bar{\chi}_d(\vec{b})} \left[ i\bar{\chi}_o - \frac{1}{2}\bar{\chi}_o^2 - \frac{1}{3!}i\bar{\chi}_o^3 + \dots \right] d^2\vec{b} \end{aligned} \quad (52)$$

The first term is the elastic coherent amplitude, the second term is the distorted wave Born approximation, and the remaining terms are multiple excitation corrections.

## BIBLIOGRAPHY

- <sup>1</sup>K. M. Watson, Phys. Rev. 89, 575 (1953).
- <sup>2</sup>M. L. Goldberger and K. M. Watson, "Collision Theory" John Wiley and Sons, NY, p. 749 (1964).
- <sup>3</sup>R. J. Glauber, Phys. Rev. 100 (1955) 242.
- <sup>4</sup>V. Franco and R. J. Glauber, Phys. Rev. 142 (1966) 1195.
- <sup>5</sup>Larry Zamick, Ann. Phys. 21, 550 (1963).
- <sup>6</sup>Victor Franco, Phys. Rev. 175, 1376 (1968).
- <sup>7</sup>O. Kofoed-Hansen, Nuovo Cimento 60A, 621 (1969).
- <sup>8</sup>W. Czyż and L. C. Maximon, Ann. Phys. 52, 59 (1969).
- <sup>9</sup>J. W. Wilson, Phys. Lett. 52B, 149 (1974).
- <sup>10</sup>T. A. Osborn, Ann. Phys. 58 (1970) 417.
- <sup>11</sup>M. L. Goldberger and K. M. Watson, "Collision Theory" John Wiley and Sons, NY, p. 330 (1964).
- <sup>12</sup>H. Kanada, K. Sakai, and M. Yasuno, Prog. Theor. Phys. 46, 1071 (1971).
- <sup>13</sup>G. Fäldt and H. Pilkuhn, Ann. Phys. 58, 454 (1970).
- <sup>14</sup>G. Alberi, L. Bertocchi, and G. Bialkowski, Nucl. Phys. 17, 621 (1974).
- <sup>15</sup>L. Bertocchi and A. Tékou, Nuovo Cimento 12A, 1 (1972).
- <sup>16</sup>A. Tékou, Nucl. Phys. B46, 141 (1972).
- <sup>17</sup>J. Formánek, Nucl. Phys. B12, 441 (1969).
- <sup>18</sup>A. Tékou, Nucl. Phys. B46, 152 (1972).
- <sup>19</sup>G. Fäldt, H. Pilkuhn, and H. G. Schlaile, Ann. Phys. 82, 326 (1974).
- <sup>20</sup>P. B. Jones, "The Optical Model in Nuclear and Particle Physics" Interscience Publishers, New York, 1963, pp. 11,72.
- <sup>21</sup>I. Ulehla, L. Gomolcak, and Z. Pluhar, "Optical Model of the Atomic Nucleus," Academic Press, NY, p. 11 (1964).

- <sup>22</sup>N. C. Francis and K. M. Watson, Phys. Rev. 92 (1953) 291.
- <sup>23</sup>A. K. Kerman, H. McManus, and R. M. Thaler, Ann. Phys. 8 (1959) 551.
- <sup>24</sup>A. Dar and Z. Kirzon, Phys. Lett. 37B 166 (1971).
- <sup>25</sup>G. F. Chew, Large and Small Baryon Numbers in High Energy Collision Theory, University of California (Berkeley) Preprint, May 21, 1973.
- <sup>26</sup>G. F. Chew, The Analytic S Matrix, W. A. Benjamin, New York, 1966.
- <sup>27</sup>R. J. Eden, "High-Energy Collisions of Elementary Particles" Cambridge University Press, London, 1967, chpt. 5.
- <sup>28</sup>M. Gell-Mann, Phys. Rev. Lett. 8 (1962) 263.
- <sup>29</sup>V. N. Gribov and I. Ya. Pomeranchuk, Phys. Rev. Lett. 8 (1962) 343.
- <sup>30</sup>B. M. Udgoankar and M. Gell-Mann, Phys. Rev. Lett. 8 (1962) 346.
- <sup>31</sup>V. N. Gribov, Sov. J. Nucl. Phys. 9 (1969) 369.
- <sup>32</sup>P. M. Fishbane and J. S. Trefil, Phys. Rev. Lett. 32 (1974) 396.
- <sup>33</sup>V. Franco, Phys. Rev. Lett. 32 (1974) 911.
- <sup>34</sup>W. L. Wang, Phys. Lett. 52B (1974) 143.
- <sup>35</sup>T. T. Chou and C. N. Yang, Phys. Rev. 170 (1968) 1591.
- <sup>36</sup>M. L. Goldberger and K. M. Watson, "Collision Theory" John Wiley and Sons, NY, p. 683 (1964).
- <sup>37</sup>D. R. Harrington, Phys. Rev. 184 (1969) 1745.
- <sup>38</sup>L. L. Foldy and J. D. Walecka, Ann. Phys. 54, 447 (1969).
- <sup>39</sup>R. Hofstadter and H. R. Collard, Nuclear Radii Determined by Electron Scattering, Landolt-Börnstein Series, Vol. 2, Springer-Verlag, Berlin-Heidelberg-New York, (1967).
- <sup>40</sup>W. Schimmerling, T. J. Devlin, W. W. Johnson, K. G. Vosburgh, and R. E. Mischke, Phys. Lett. 37B, 177 (1971).

- <sup>41</sup>W. Schimmerling, T. J. Devlin, W. W. Johnson, K. G. Vosburgh, and R. E. Mischke, Phys. Rev. C7, 248 (1973).
- <sup>42</sup>V. S. Barashenkov, K. K. Gudima, and V. D. Toneev, Fort. Phys. 17 (1969) 683.
- <sup>43</sup>G. I. Igo, J. L. Friedes, H. Palevsky, R. Sutter, G. Benett, W. D. Simpson, D. M. Corlet, and R. L. Stearns, Phys. Rev. Lett 18 (1967) 1200.
- <sup>44</sup>G. P. Millburn, W. Birnbaum, W. E. Crandell, and L. Schechter, Phys. Rev. 95 (1954) 1268.
- <sup>45</sup>H. H. Heckman, P. Linstrom, D. Griener, F. S. Beiser, and B. Cork, Bull. Am. Phys. Soc. 19, 518 (1974).
- <sup>46</sup>G. F. Chew, Phys. Rev. 84 (1951) 1057.
- <sup>47</sup>K. M. Watson, Phys. Rev. 89 (1953) 575.
- <sup>48</sup>M. E. Best, Can. J. Phys. 50 (1972) 1609.
- <sup>49</sup>N. Austern, Direct Reaction Theories, in "Fast Neutron Physics Part II, Ed. by J. B. Marion and J. L. Fowler (Interscience Publishers, New York, 1963) p. 1113.
- <sup>50</sup>M. L. Goldberger and K. M. Watson, Collision Theory (John Wiley and Sons, New York, 1964) p. 818.



## VITA

### JOHN WILLIAM WILSON

He was born of farming parents in Arkansas City, Kansas, on August 6, 1940. He attended Lincoln Elementary and subsequently graduated from Arkansas City Junior High (1955), Arkansas City Senior High (1958), and Arkansas City Junior College (1960) where he was introduced to physics as a career. He attended Southwestern College (summer 1960) and obtained a B.S. in physics from Kansas State University (1962). He attended graduate school at KSU before accepting a position as an aerospace technologist at the NASA, Langley Research Center (1963). He attended courses of the Virginia Polytechnic Institute (1964) and developed numerical techniques for real-time digital flight simulation, new methods for the simulation of rotational dynamics, and new methods for rotational visual display systems which avoid mechanical locking (four-gimbal). He entered the College of William and Mary (1965), became a Ph.D. candidate (1967), and received an M.S. in physics (1969). During this period, his professional efforts changed from flight simulation to high-energy nucleon transport and the study of the radiation hazards to high-altitude aircraft and spacecraft. He predicted the importance of high-energy secondary-atmospheric neutrons which has been subsequently verified by recent experiments. His first thesis topic, Nucleon-Deuteron Scattering Theory, was not completed. He has authored over 35 technical and scientific papers of which 13 are on the subject of high-energy nuclear reaction theory.

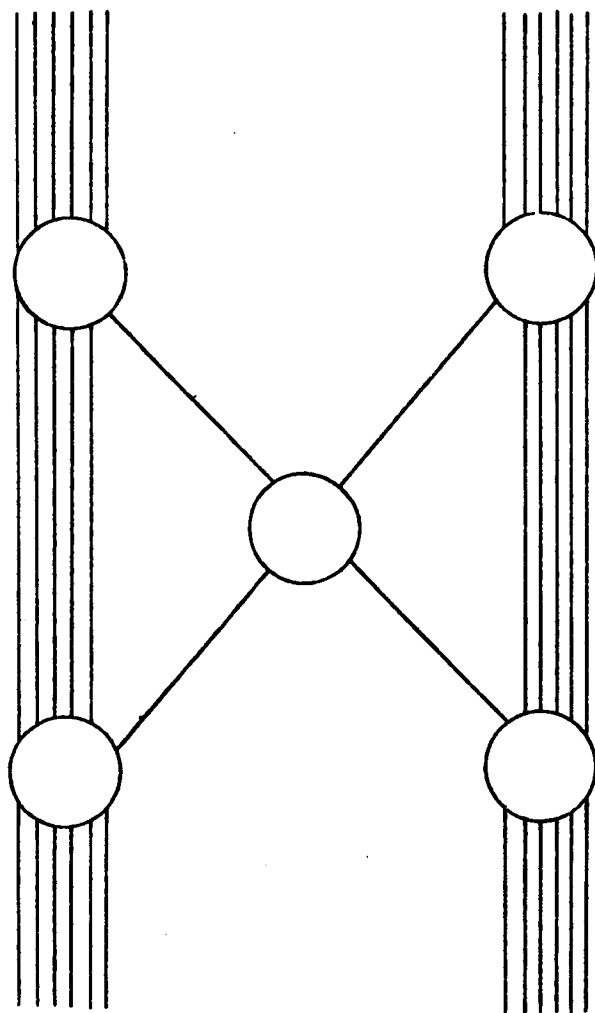


Fig. 1. Single scattering graph.

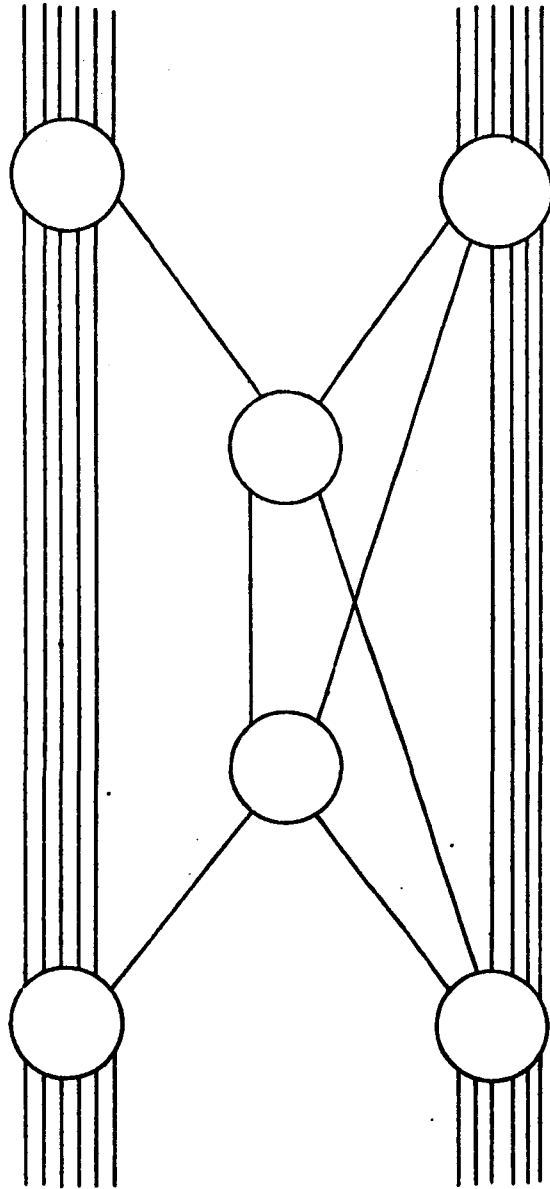


Fig. 2. Rescattering graphs.

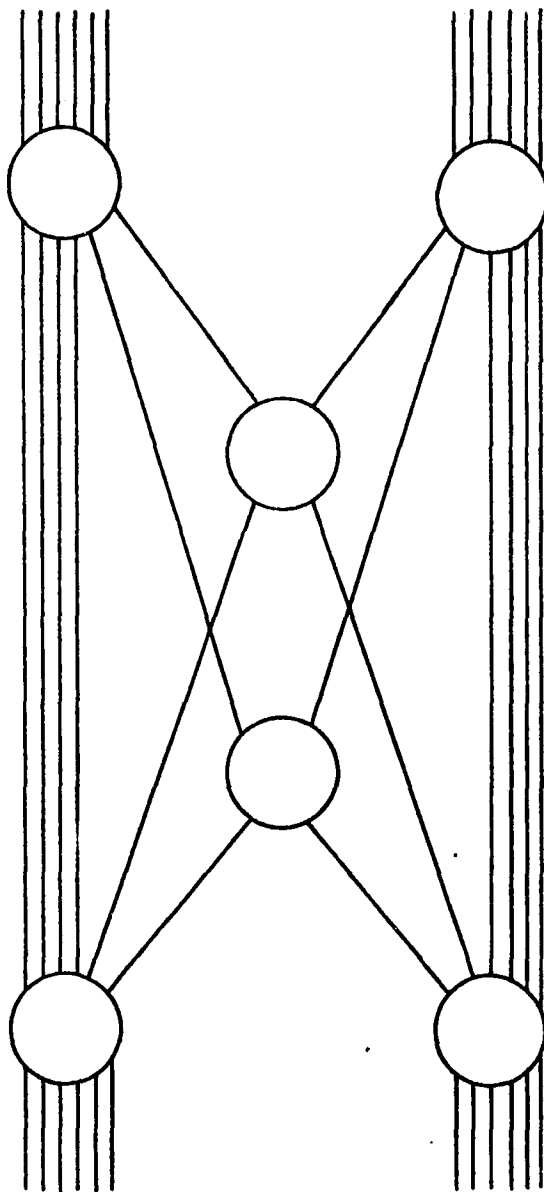


Fig. 2. Continued.

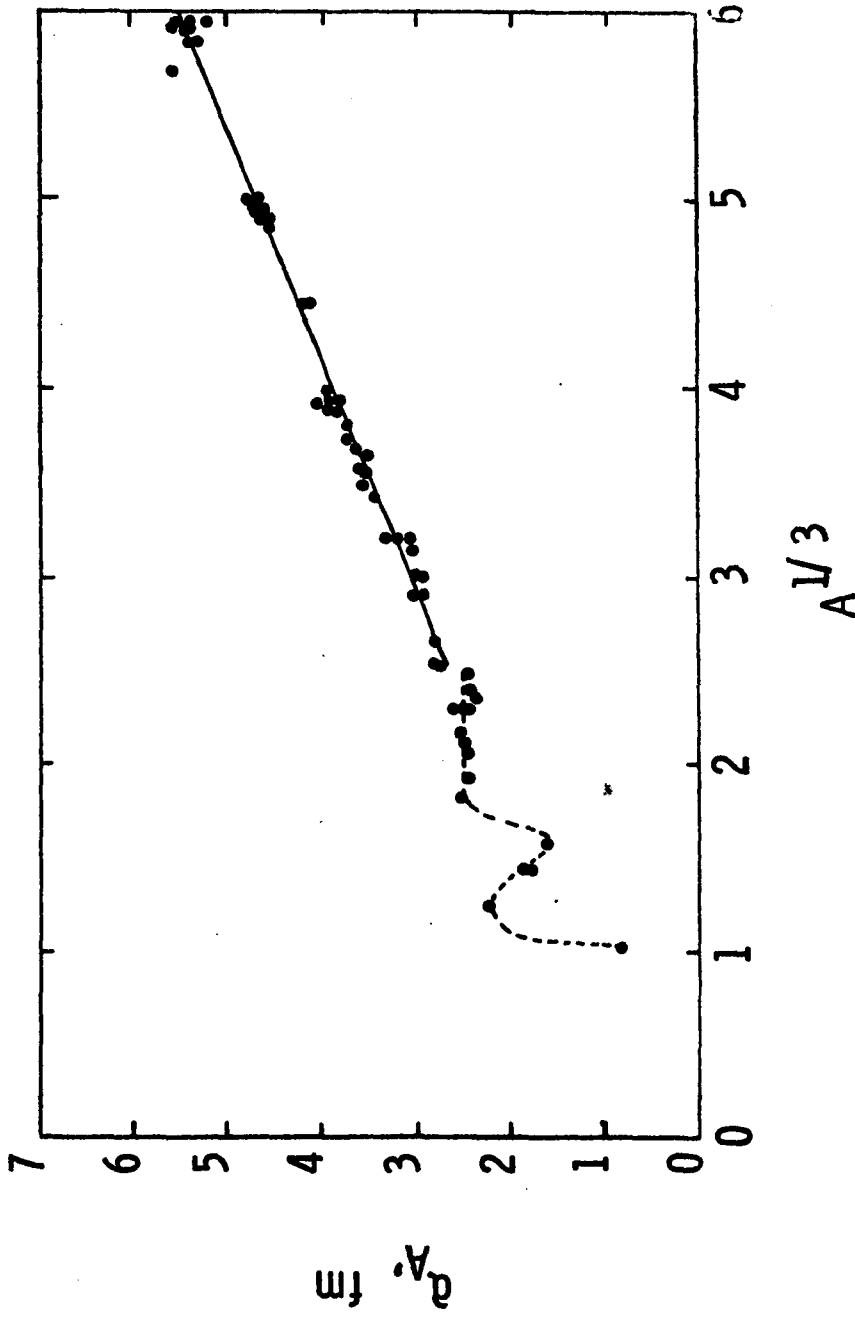


Fig. 3. Nuclear root-mean-square radius as a function of mass number. Dashed curve is to guide the eye thru values used in calculations. Solid curve is used above 016. Dots are data tabulated by Hofstadter and Collard.

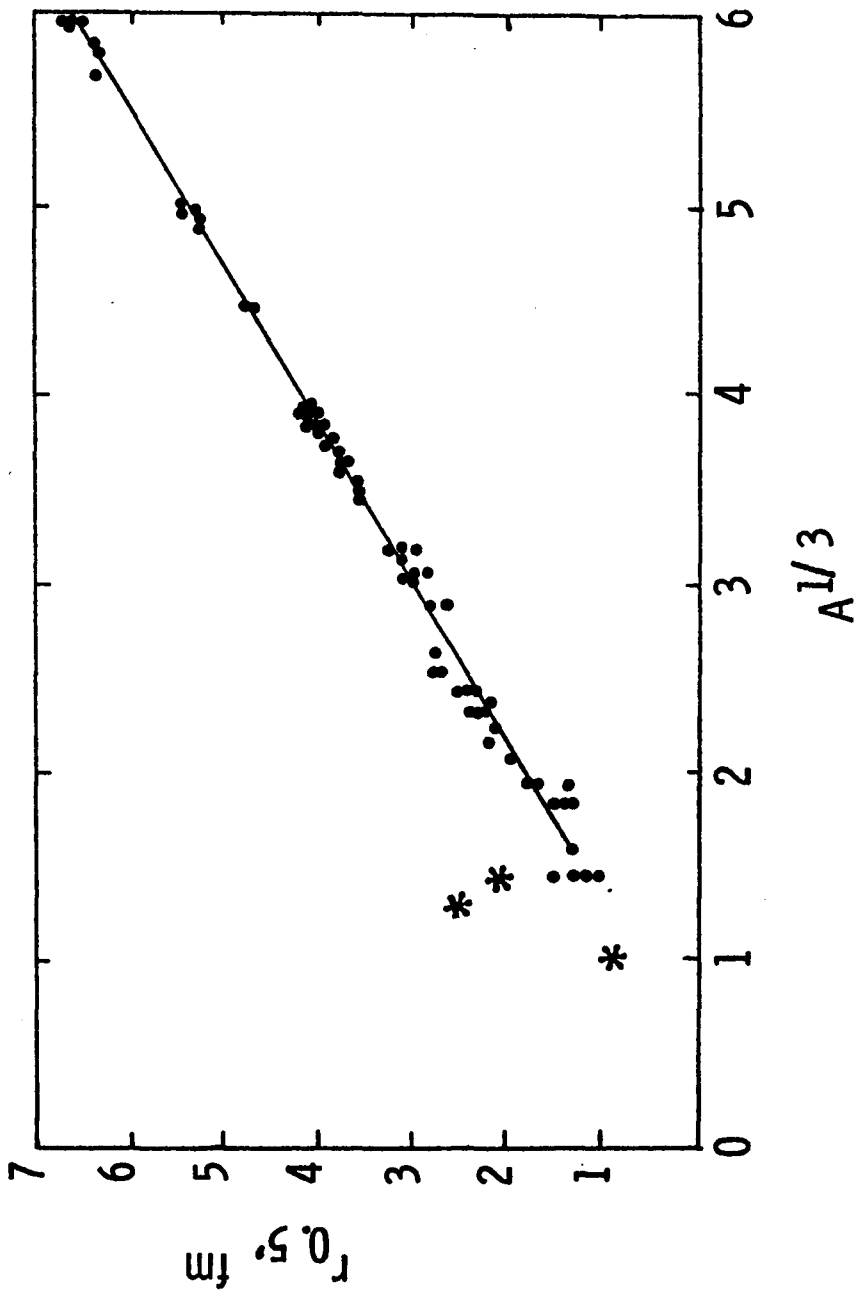


Fig. 4. Nuclear half-density radius as a function of mass number. Solid curve is used above  $\text{He}^4$ . Stars are values below  $\text{He}^4$  obtained from assumed Gaussian density. Dots are data tabulated by Hofstadter and Collard.

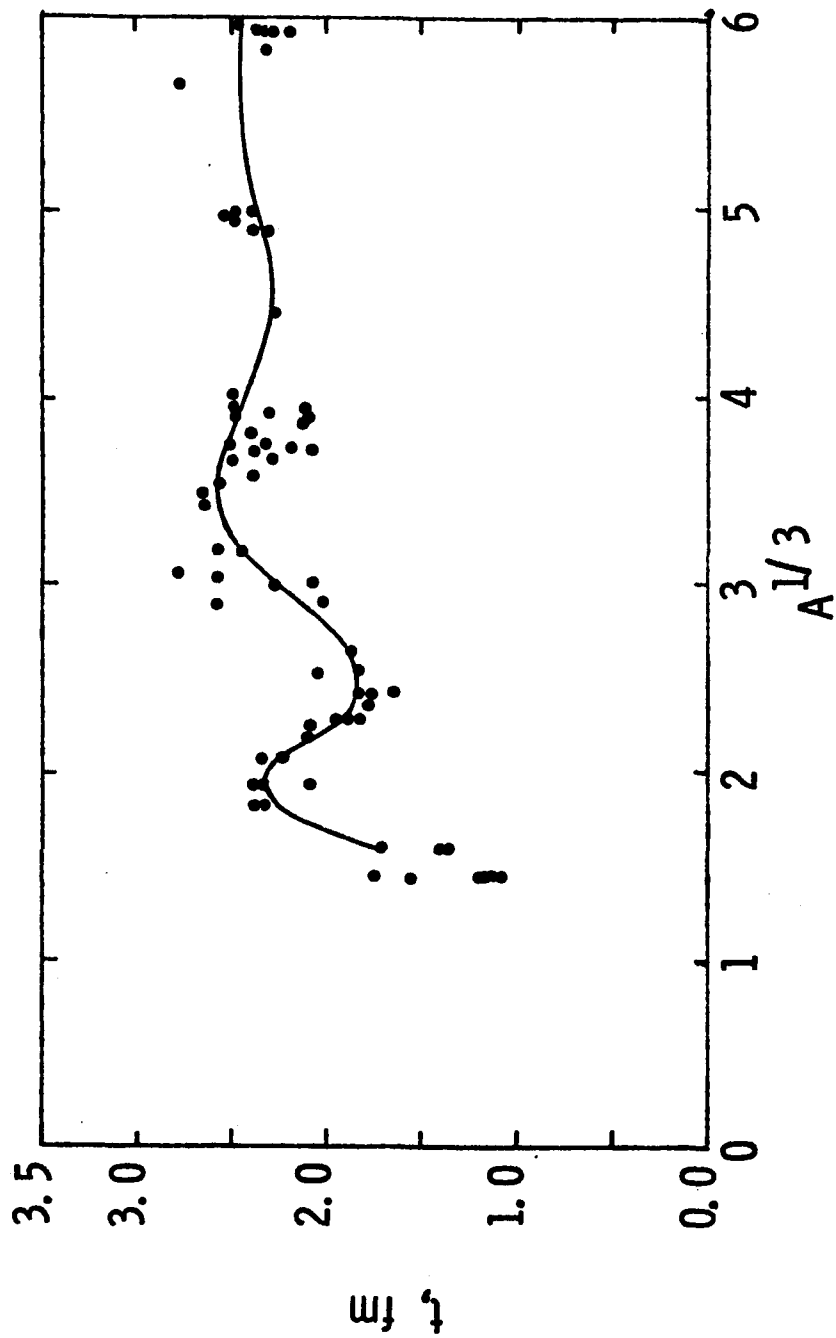


Fig. 5. Nuclear skin thickness as a function of mass number. Solid curve is used above  $\text{He}^4$ . Dots are data tabulated by Hofstadter and Collard.

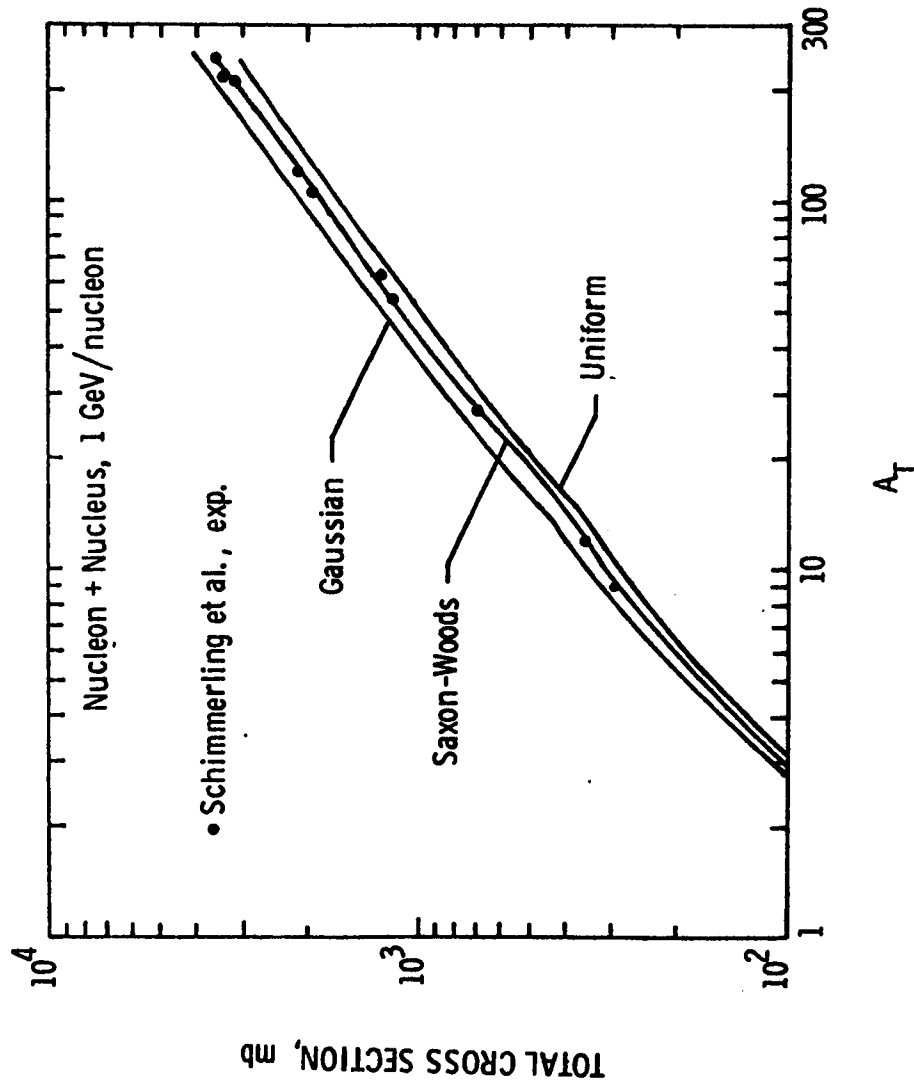


Fig. 6. Total nucleon-nucleus cross section as a function of nuclear mass number for three model single-particle densities. Dots are data for neutron scattering at 1.064 GeV obtained by Schimmerling et al.



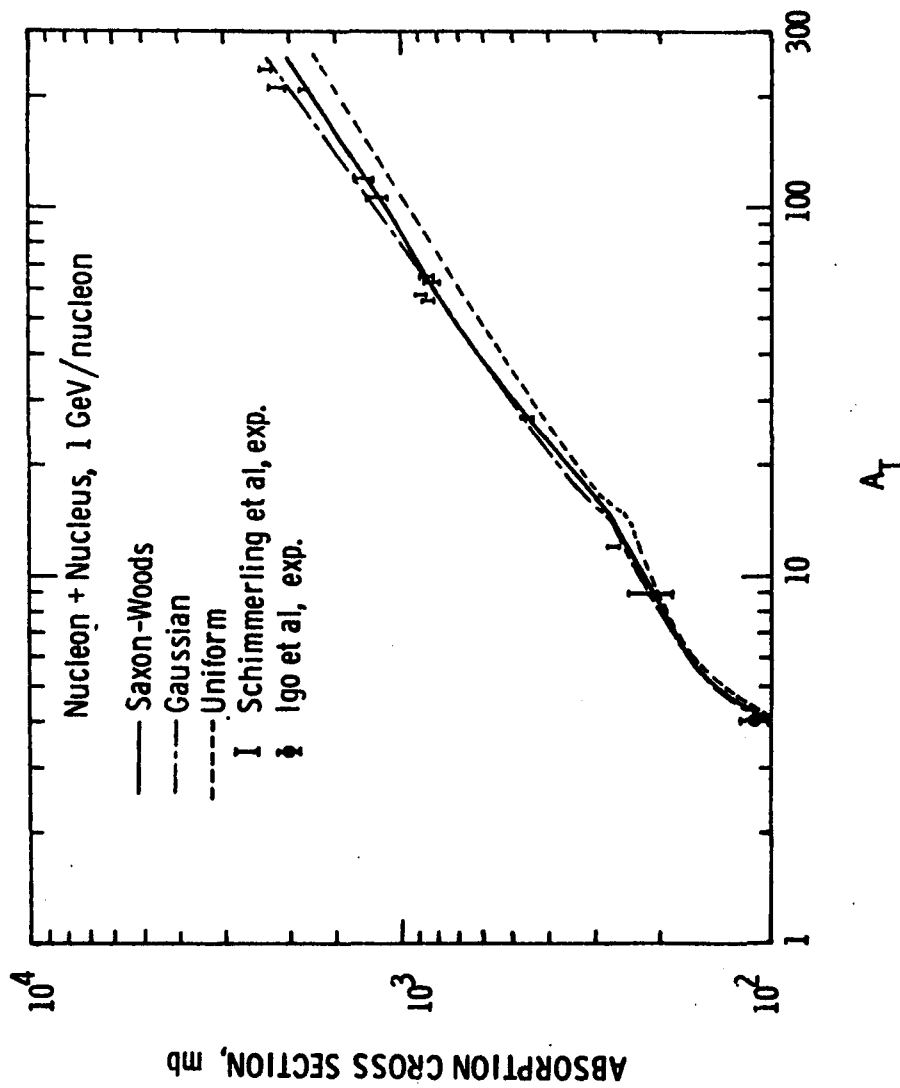


Fig. 7. Nucleon-nucleus absorption cross section as a function of nuclear mass number for three model single-particle densities in comparison of experimental data at about 1 GeV.

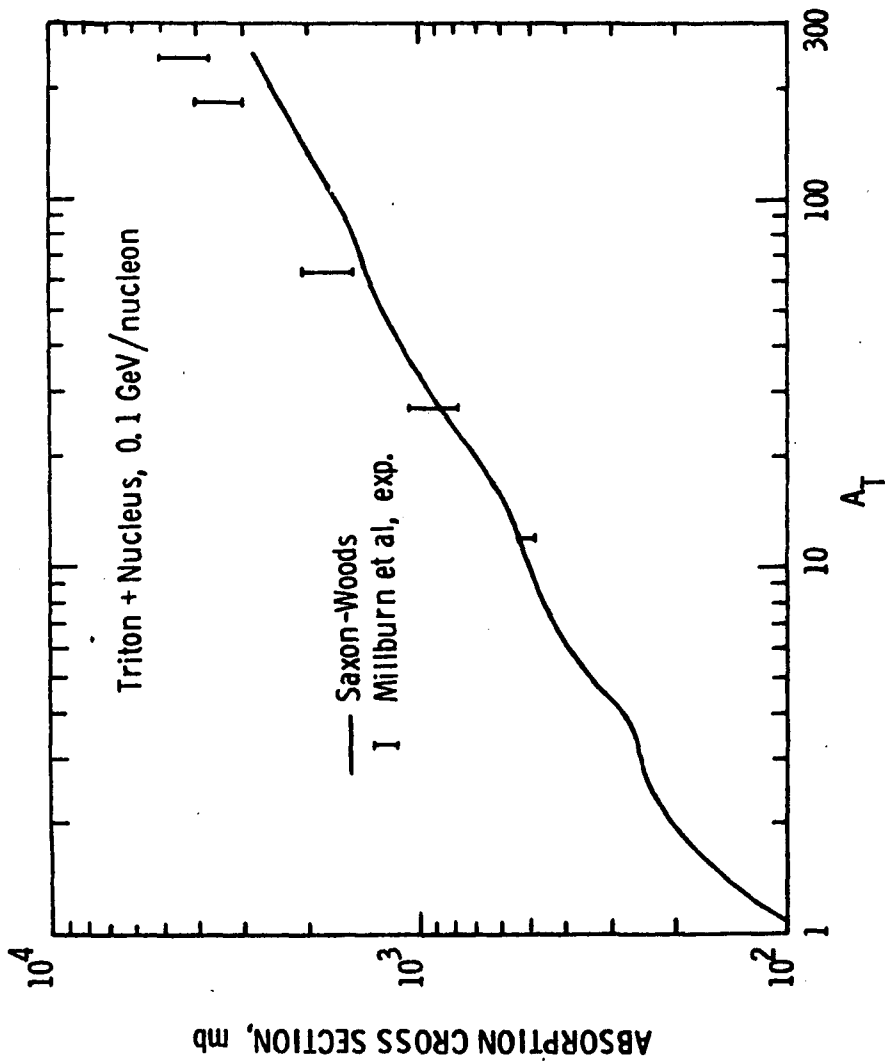


Fig. 8. Triton-nucleus absorption cross section as a function of target mass number for Saxon-Woods single-particle densities in comparison to measurements of Millburn et al. at 100 MeV/nucleon.

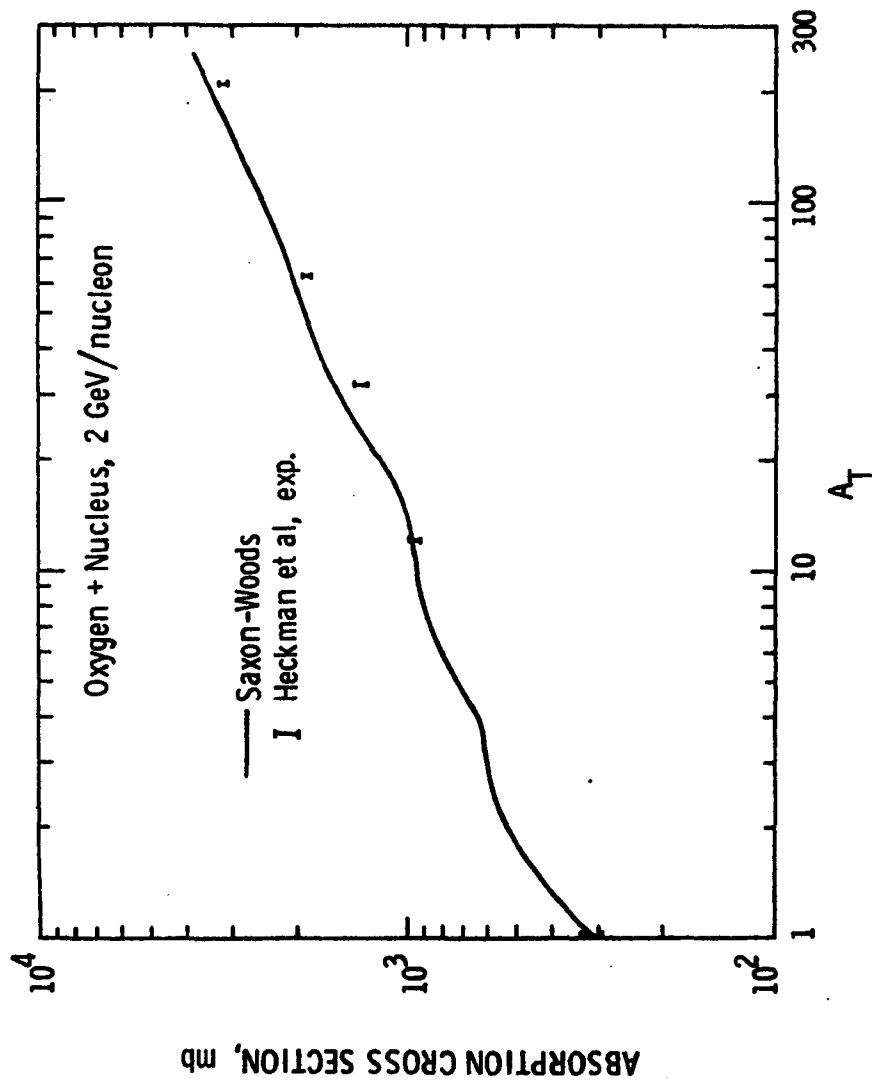


Fig. 9. Oxygen-nucleus absorption cross sections as a function of target mass number for Saxon-Woods single-particle densities in comparison to measurements of Heckman et al. at 2.1 GeV/nucleon.

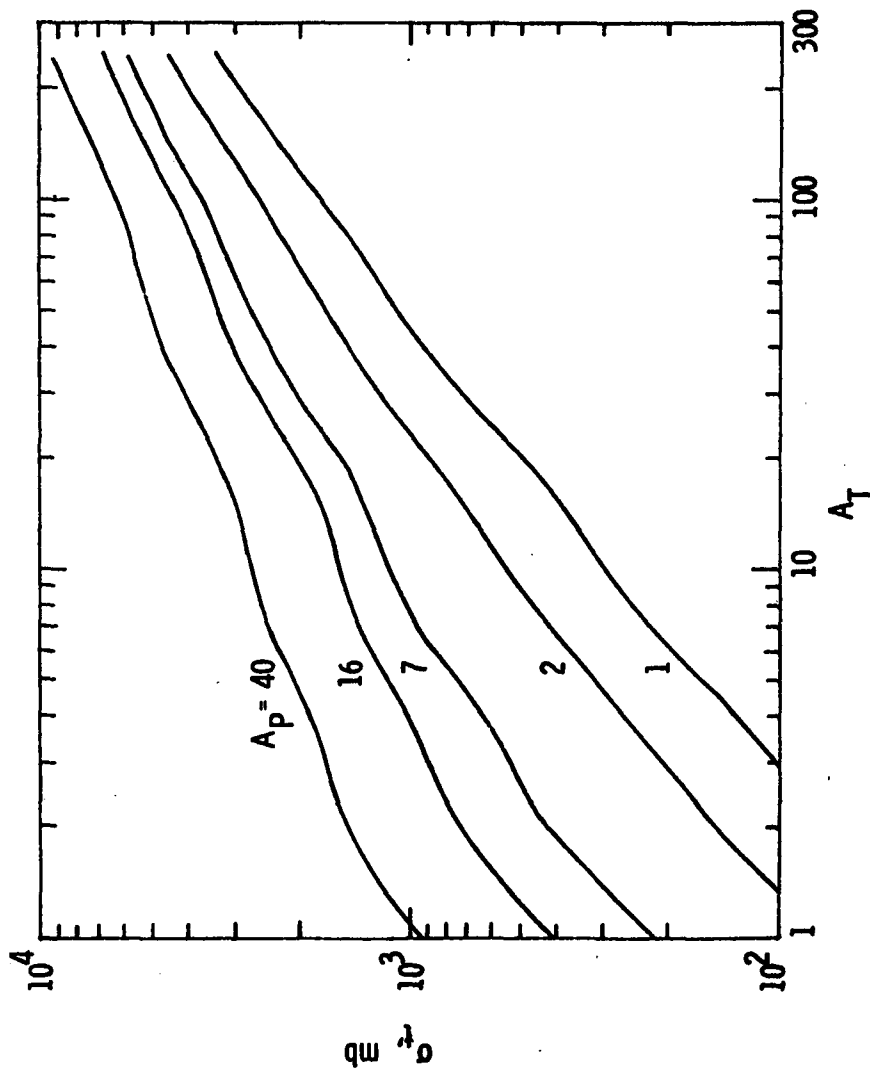


Fig. 10. Total cross section as a function of projectile and target mass numbers for 1 GeV/nucleon using the Saxon-Woods single-particle densities.

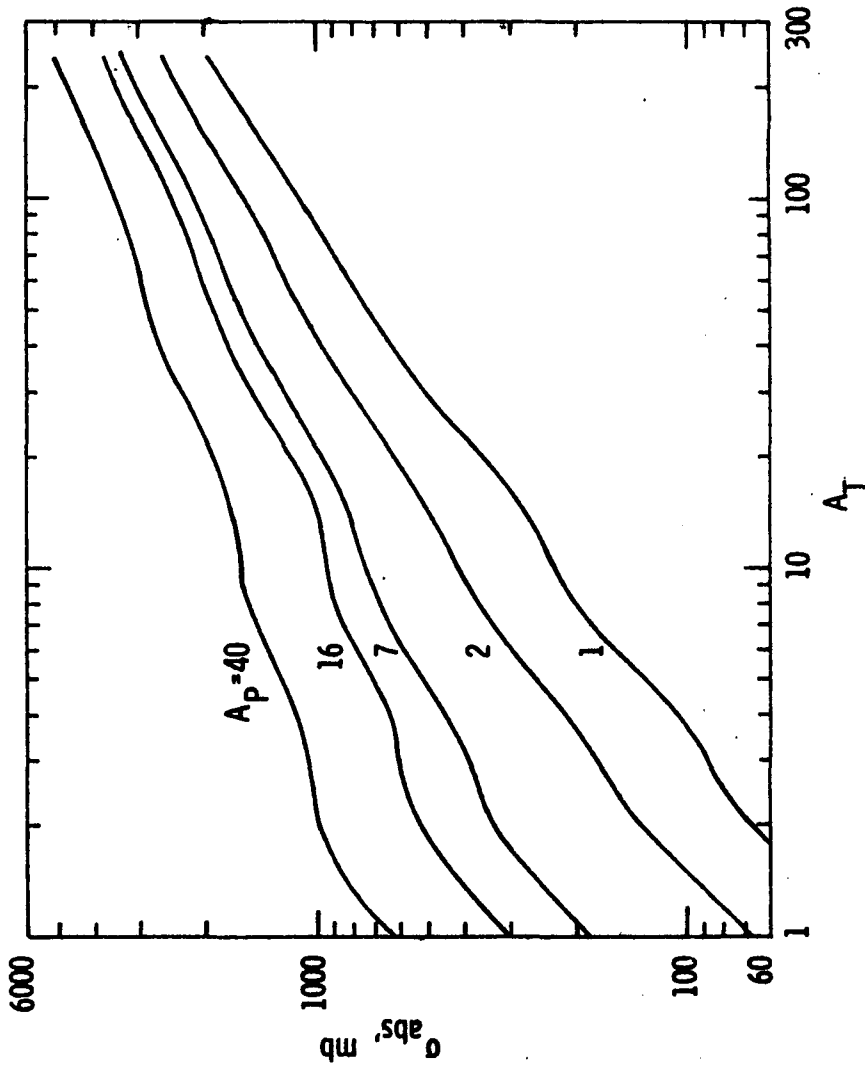


Fig. 11. Absorption cross section as a function of projectile and target mass numbers for 1 GeV/nucleon as calculated using Saxon-Woods single-particle densities.

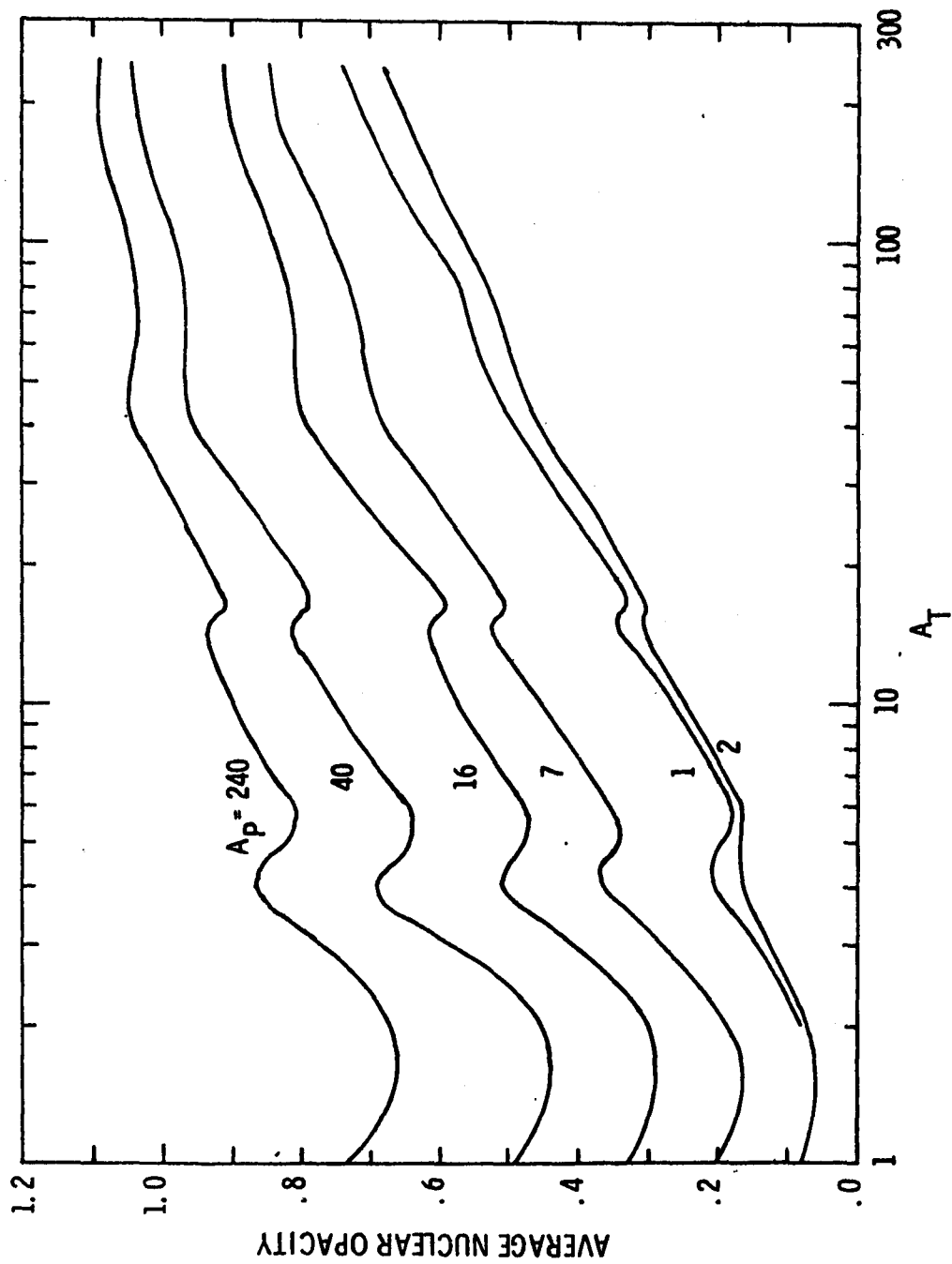


Fig. 12. Average nuclear opacity as a function of projectile and target mass numbers for 1 GeV/nucleon as calculated using Saxon-Woods single-particle densities and equivalent uniform radii given by Hofstadter and Collard.

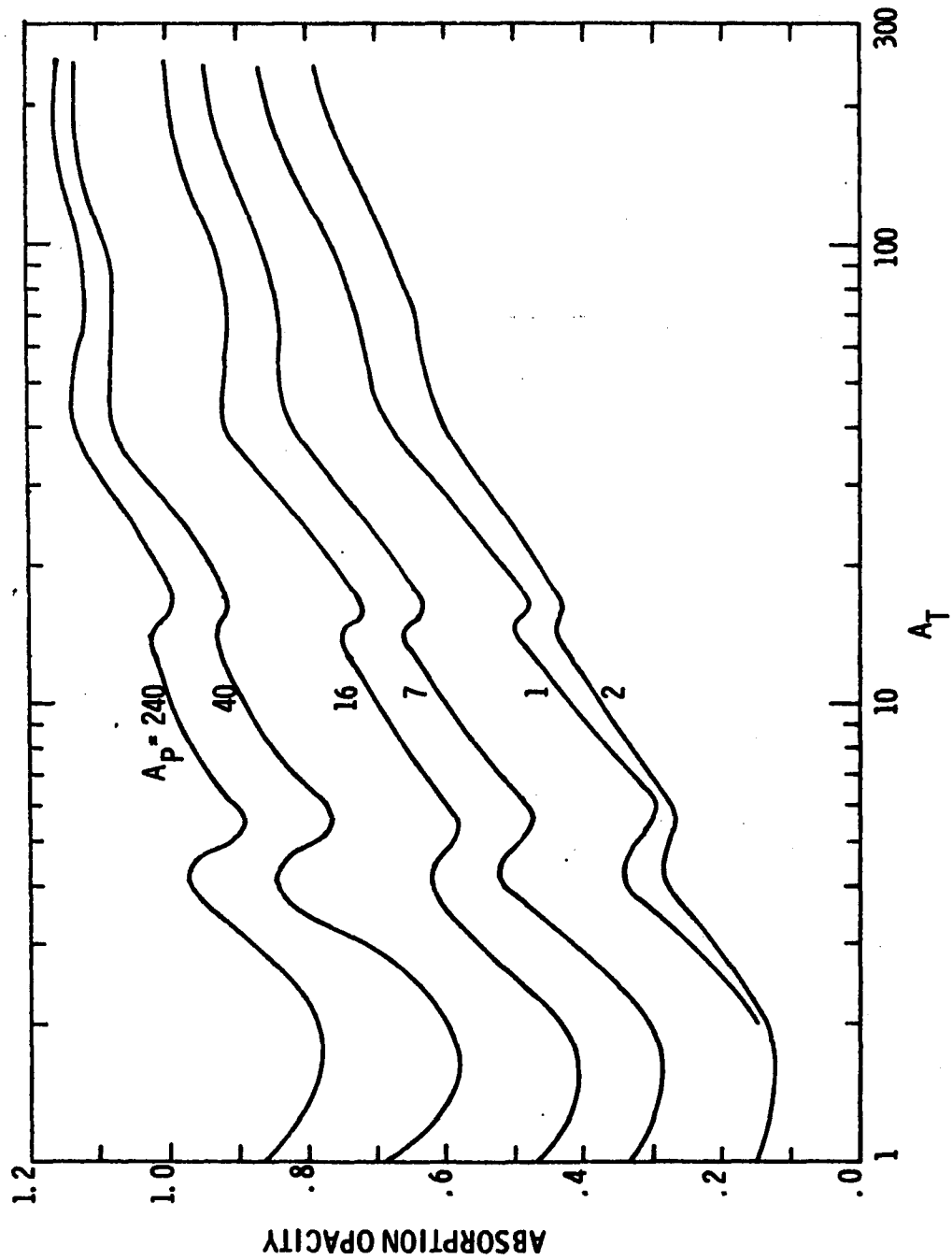


Fig. 13. Absorption nuclear opacity as a function of projectile and target mass numbers for 1 GeV/nucleon as calculated using Saxon-Woods single-particle densities and equivalent uniform radii given by Hofstadter and Collard.

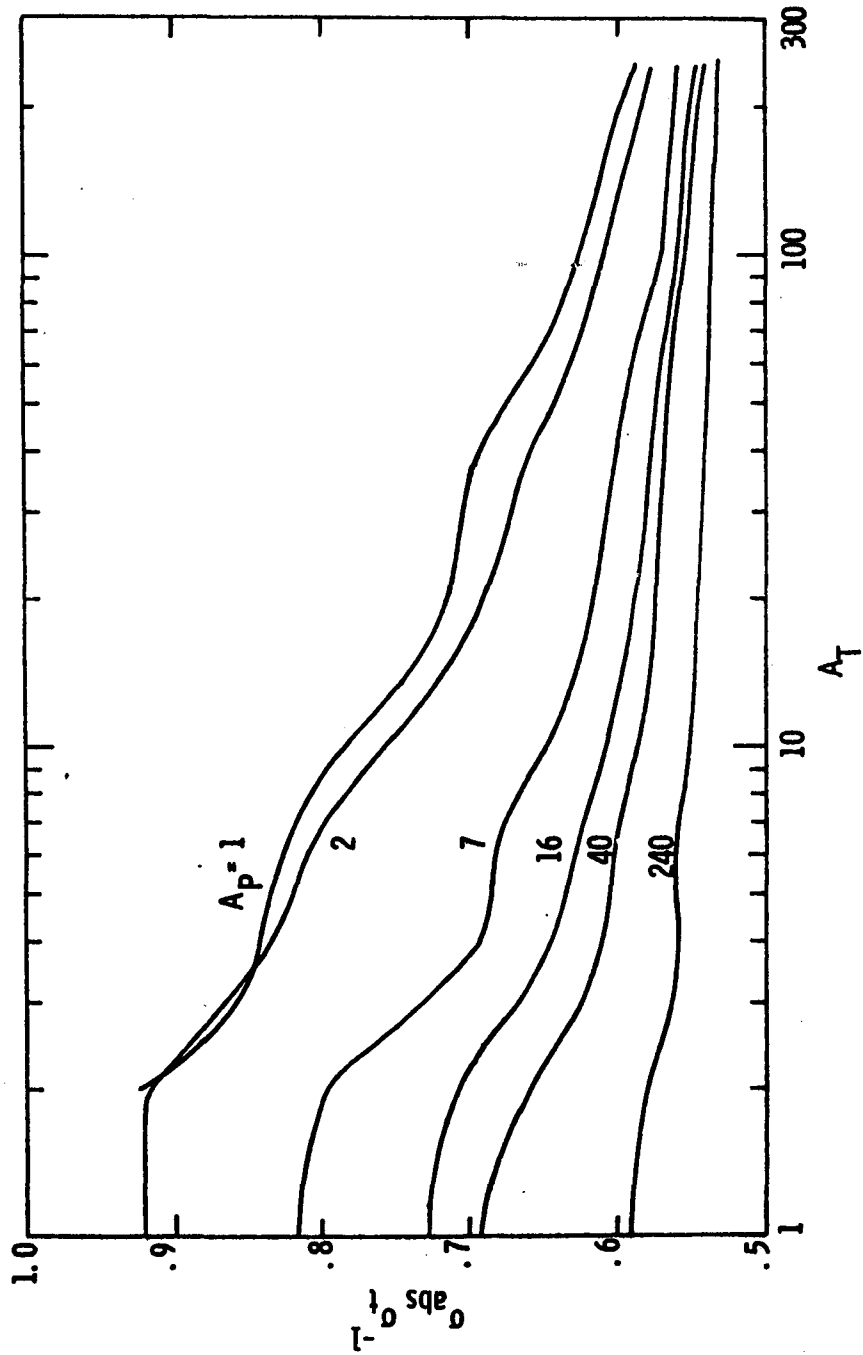


Fig. 14. Absorption to total cross section ratio as a function of projectile and target mass numbers for 1 GeV/nucleon.



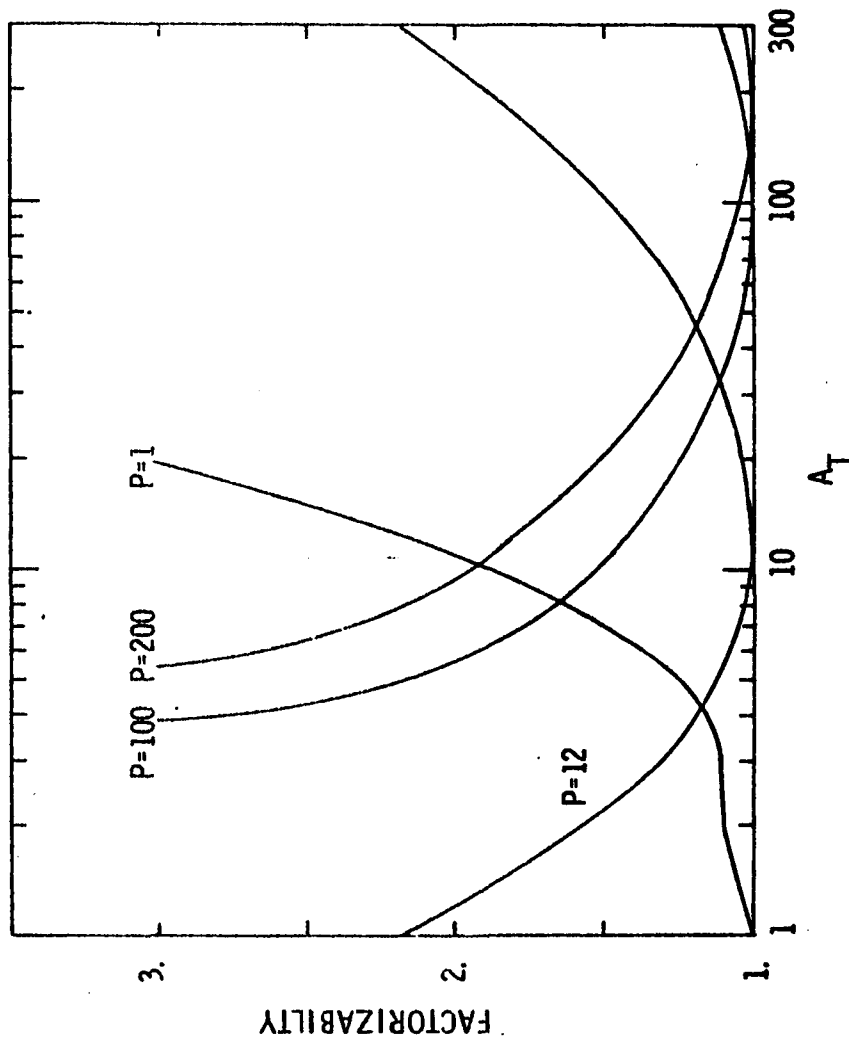


Fig. 15. Factorizability as a function of projectile and target mass numbers for 1 GeV/nucleon.